CHAPTER IV

RESULTS AND DISCUSSION

In this research, zeolite beta/Al-HMS composite catalyst has been synthesized using well-crystallized zeolite beta. The prepared composite catalyst was characterized by X-ray diffraction, SEM, solid state ^{27}Al-NMR and N_2 adsorption technique and investigated the activity in cracking processes of lubricant oil, grease and polypropylene.

4.1 The physical properties of catalysts

4.1.1 XRD pattern of zeolite beta

Synthesis of zeolite beta (Si/Al = 60) with the mole ratio in gel of $1SiO_2$: 0.0083 Al_2O_3: 0.73 TEAOH: 19 H_2O was reported by J. Aguado *et al.* [61]. The powder XRD patterns of as-synthesized and calcined zeolite beta were shown in Figure 4.1. The broad diffraction peak of (101) plane was observed in the 2θ range of 6.5-8.5° indicating the presence of two isomorphs, A and B, in zeolite beta . The most intense sharp peak at 22.4° was assigned to the diffraction of (302) plane, suggesting the high crystallinity of the zeolite. The intensity of (302) peak at 22.4 ° was decreased due to dealumination of aluminum from the tetrahedral framework. This result is in agreement with J. Aguado *et al.* [61].

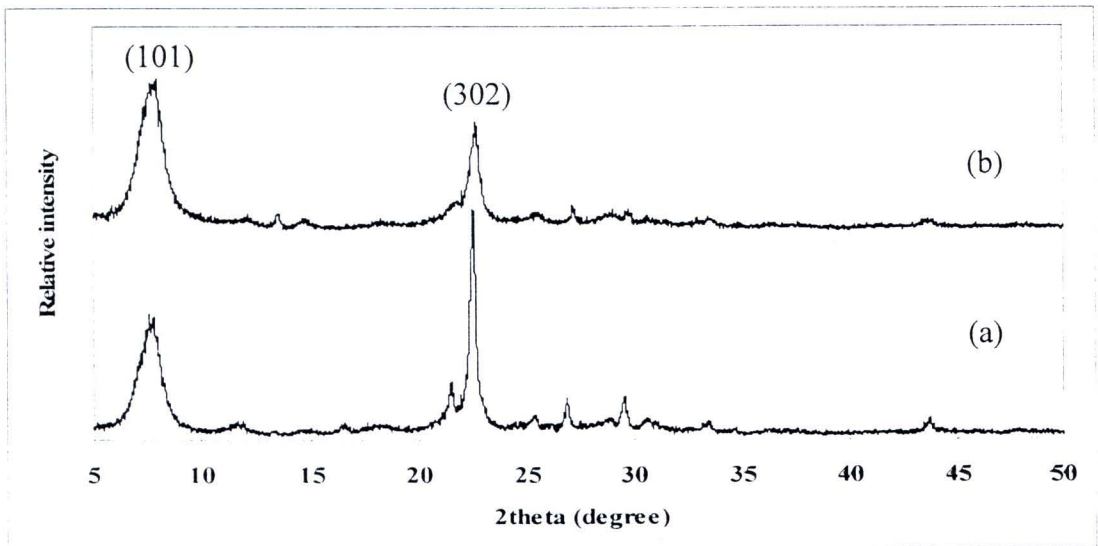

Figure 4.1 XRD patterns of (a) as-synthesizd and (b) calcined zeolite beta (Si/Al=60).

4.1.2 XRD pattern of Al-HMS

Aluminum-containing hexagonal mesoporous silica (Al-HMS) with the Si/Al mole ratios in gel of 60 were synthesized with the gel mole composition of $1SiO_2$: 0.00833 Al_2O_3: 0.25 HDA: 8.3 EtOH: 100 H_2O reported by Tuel *et al* [46]. XRD pattern of calcined Al-HMS was shown in Figure 4.2. A broad reflection peak of (100) at the 2θ range of 1.0–2.0° indicated the hexagonal mesoporous structure of HMS. Considering the calcined sample, the diffraction pattern of (100) peak was slightly shifted to higher angle than as-synthesized sample due to the shrinkage during the calcination process.

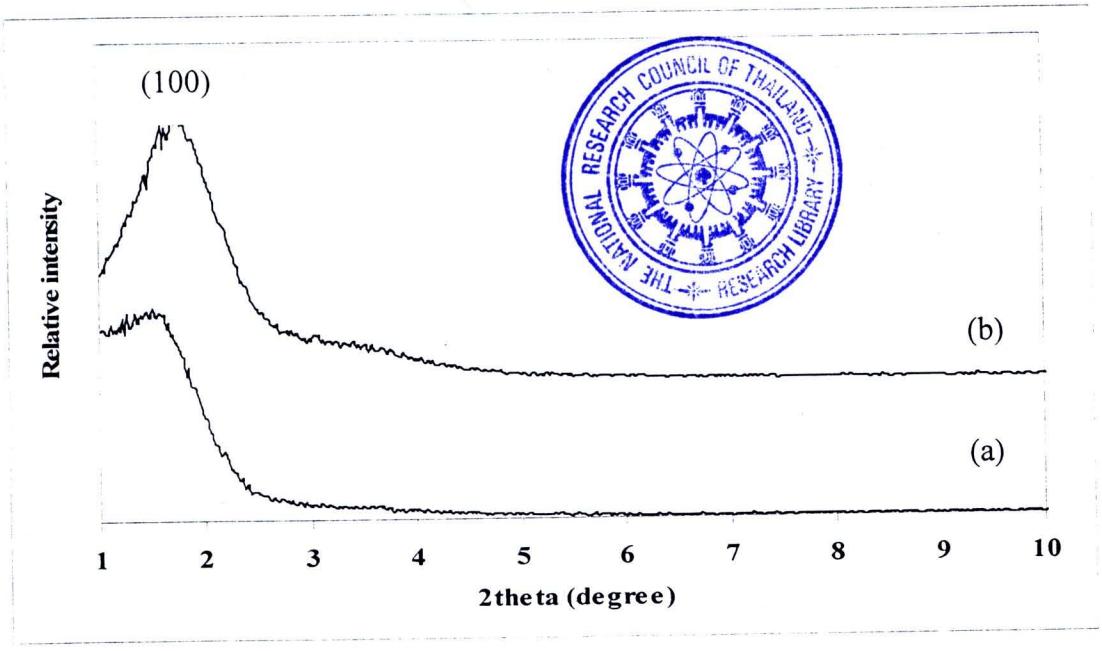

Figure 4.2 XRD patterns of (a) as-synthsized and (b) calcined Al-HMS (Si/Al=60).

4.1.3 XRD pattern of zeolite beta/Al-HMS composite

4.1.3.1 Effect of crystallization time on composite materials

Zeolite beta/Al-HMS composite with Si/Al mole ratio in gel of zeolite beta of 60 was successively synthesized using well-crystallized zeolite beta. Zeolite beta was crystallized for 72 h and dissolved in 1 M NaOH for 15 min prior the addition of HMS template for composite preparation. Then, the crystallization time of the composite was varied for 12-46 h at room temperature. The XRD patterns of as-synthesized zeolite beta/Al-HMS in Figure 4.3 indicated two distinct types of

structure. At small angle, the characteristic peak of HMS structure was observed at 2θ around 1.6 degree [46]. Whereas the broad diffraction peak of (101) plane of zeolite beta structure was observed at wide angle in the 2θ range of 7.0-8.5° and 22.4°. The diffraction at 7.0-8.5° was indicated the presence of two isomorphs, A and B, in zeolite beta. The most intense sharp peak at 22.4° was assigned to the diffraction of (302) plane, suggesting the high crystallinity of the zeolite. With increasing the crystallization time of composite materials from 12 to 16, 20 and 30 h, the zeolite beta structure were only observed with the decreasing of crystallinity. At 36 h and 46 h, the composite showed both HMS and zeolite beta structures but the crystallinity at 46 h was less than at 36 h. Then, the 36 h composite was chosen for calcination. After calcination in air at 500°C for 5 h to remove template, the HMS structure was remained and the peak intensity was increased as shown in Figure 4.3A. On the contrary, the intensity of zeolite beta peak at 22.4° was decreased due to dealumination of aluminium from the tetrahedral framework, Figure 4.3B. Therefore, the crystallization time on composite materials at 36 h was chosen for further study.

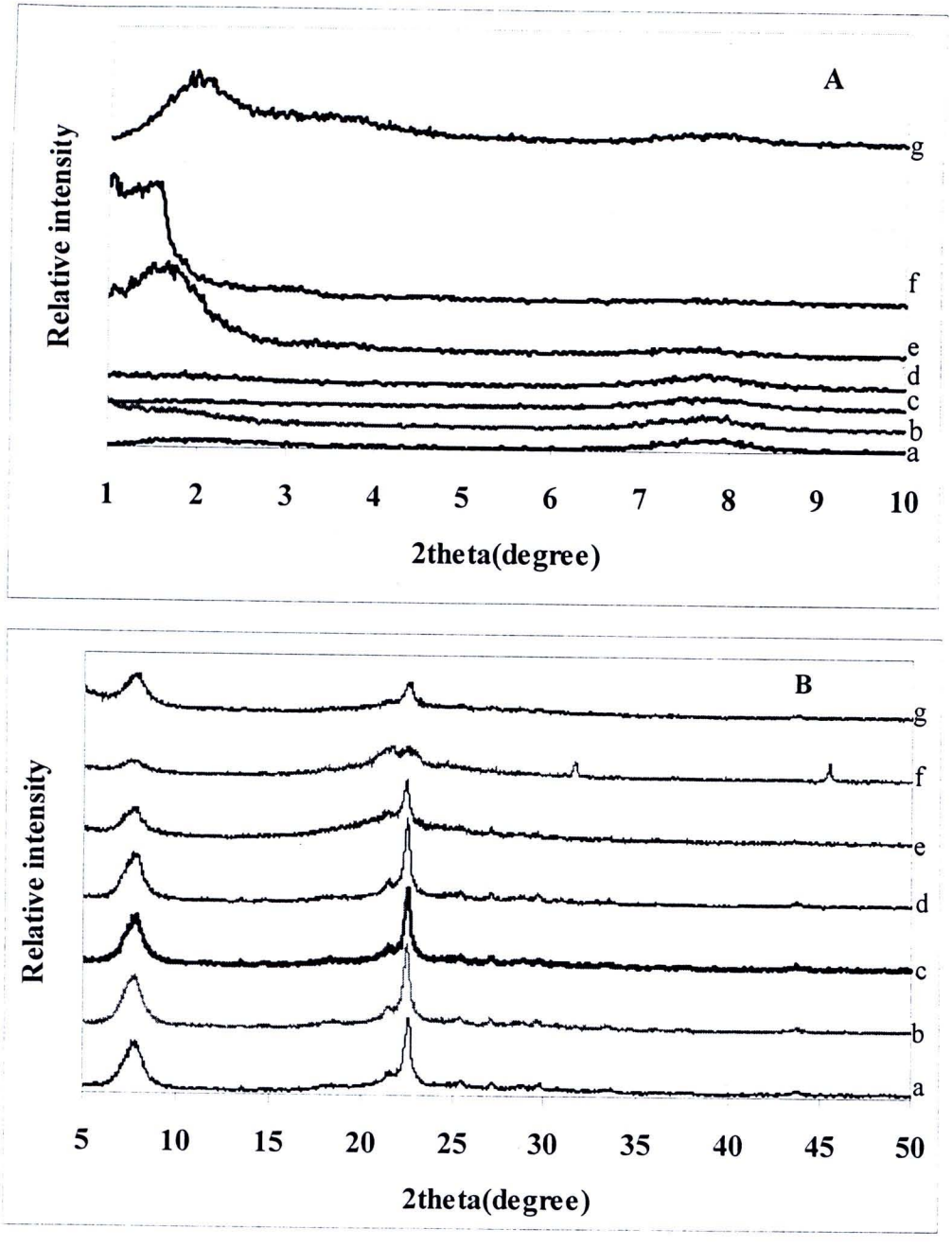

Figure 4.3 XRD patterns of as-synthesized composites at small angle (A) and wide angle (B), with various crystallization time: (a) 12h, (b) 16h, (c) 20h, (d) 30h, (e) 36h, (f) 46h, and (g) calcined composite.

4.1.3.2 Effect of NaOH concentration and time on dissolution of zeolite beta

The effect of NaOH concentration on dissolution of zeolite beta before adding the HMS template solution was studied. The concentrations of NaOH [62] were varied from 0.5 to 1 M and the dissolution time was observed for 15 and 30 min.

XRD patterns of calcined zeolite beta/Al-HMS composite in Figure 4.4 indicated the structures of HMS and zeolite beta at small angle and wide angle, respectively. The samples prepared in 1 M NaOH for 15 min and 0.5 M NaOH for 30 min provided high intensity of both structures. The result indicated that high concentration of NaOH and longer dissolution time destroyed zeolite beta structure In addition, the specific BET surface area of samples were 671, 382, and 664 m^2/g for 1 M NaOH 15 min, 1 M NaOH 30 min, and 0.5 M NaOH 30 min, respectively. Therefore, 1 M NaOH for 15 min was chosen for further study due to the crystallinity of both structures and high surface area.

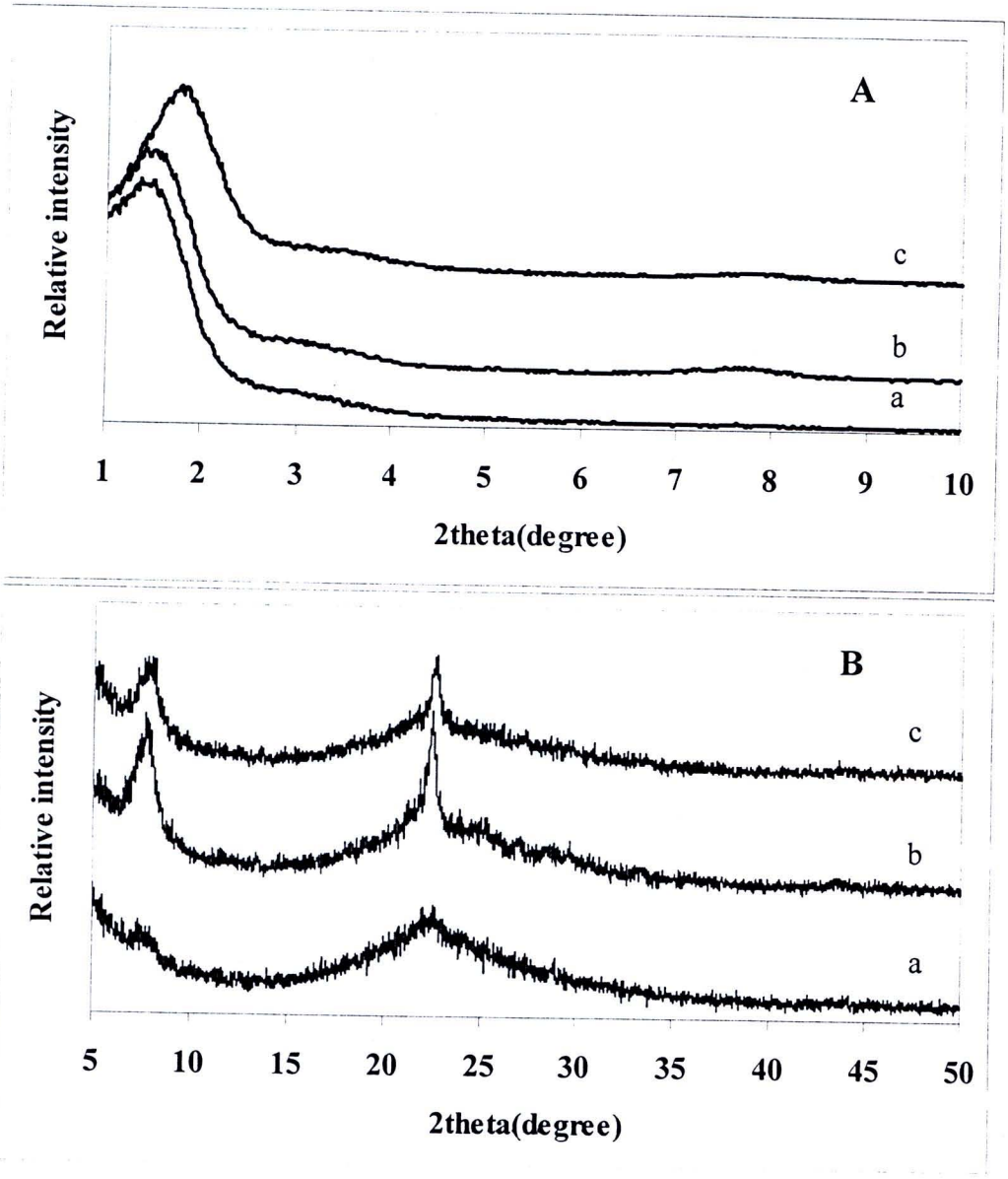

Figure 4.4 XRD patterns of calcined composite at small angle (A) and wide angle (B) in: (a) 1 M NaOH 30 min, (b) 0.5 M NaOH 30 min, and (c) 1 M NaOH 15 min.

4.1.3.3 Effect of the crystallization time of zeolite beta

The effect of crystallization time on zeolite beta at 16, 18 and 72 h [63] was studied for synthesis of zeolite beta/Al-HMS composite with Si/Al ratio in gel of zeolite beta of 60. Zeolite beta was dissolved in 1 M NaOH for 15 min before the hexadecylamine was added. All XRD patterns of calcined zeolite beta/Al-HMS composite in Figure 4.5 indicated the structures of HMS and zeolite beta at small angle and wide angle, respectively. Both XRD patterns of zeolite beta and Al-HMS exhibited high intensity at the crystallization time of 72 h. The specific BET surface areas were 497, 504 and 659 m^2/g, for crystallization time at 16, 18 and 72 h respectively. Then, the crystallization time on zeolite beta for 72 h was chosen for further study.

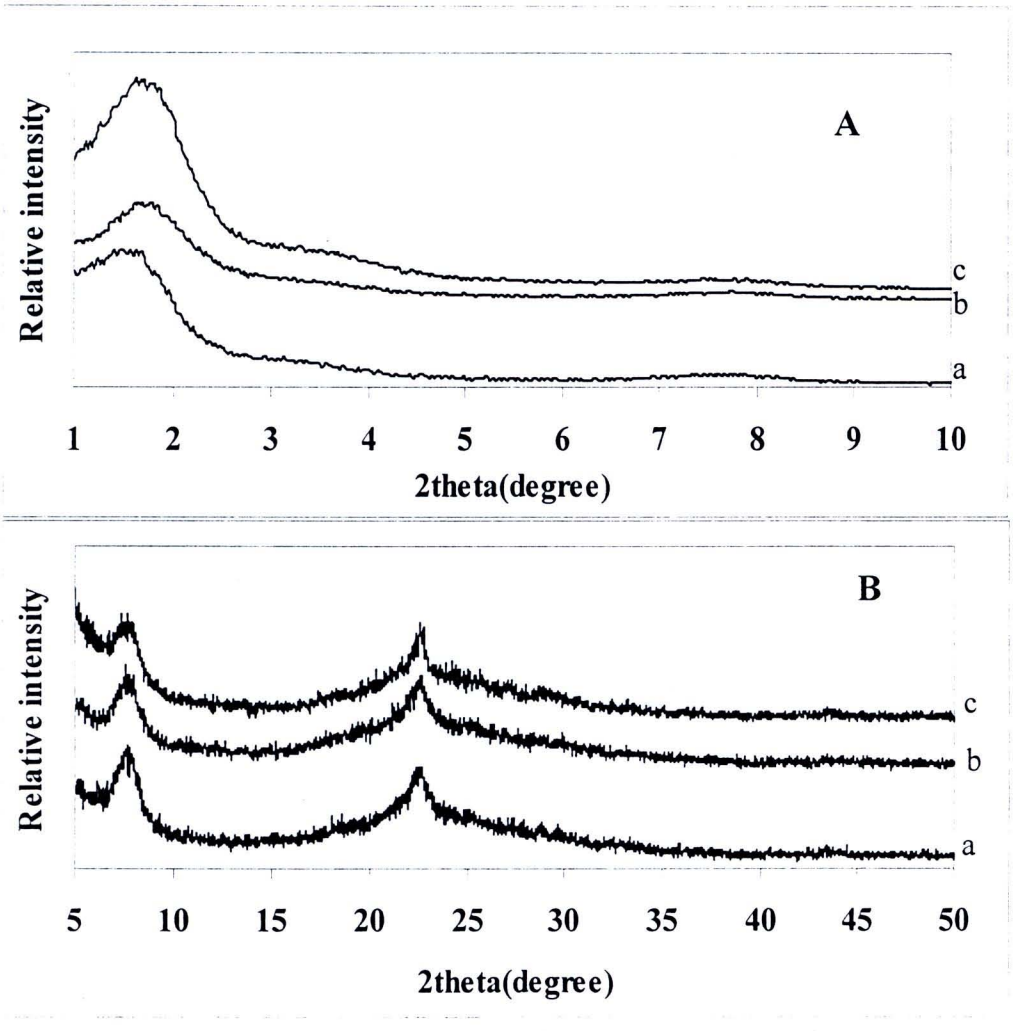

Figure 4.5 XRD patterns of calcined composite at small angle (A) and wide angle (B) in: (a) 16 h, (b) 18 h, and (c) 72 h.

4.1.3.4 Effect of Si/Al ratio

Zeolite beta/Al-HMS composite with various Si/Al ration in gel of zeolite beta (40, 60 and 120) were synthesized using crystallization time on zeolite beta at 72 h, 1 M NaOH as a dissolving solution for 15 min and crystallization time on composite material at 36 h. The XRD patterns were demonstrated in Figure 4.6. With increasing aluminum component (low Si/Al ratio), the zeolite beta structure was predominant while the HMS structure was hardly observed. This may be due to the stability of zeolite beta. The higher the aluminum contents the more stability of zeolite beta structure [64].

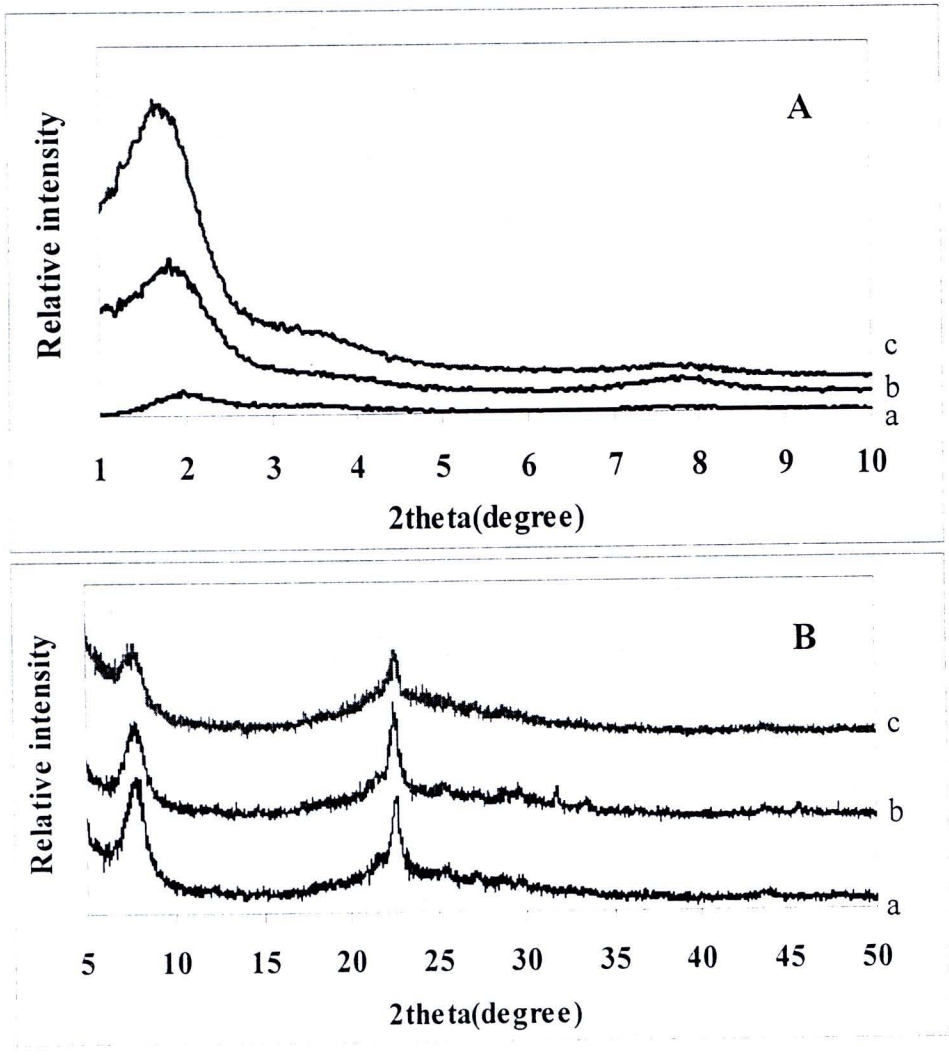

Figure 4.6 XRD patterns of calcined composite with various Si/Al ration in gel of zeolite beta of (a) 40 (b) 60 (c) 120, at small angle (A) and wide angle (B) degree.

4.1.4 SEM image of catalysts

4.1.4.1 SEM image of zeolite beta

The morphology of calcined zeolite beta was shown in Figure 4.7 Ordered round granular and shape of zeolite beta was observed with the average size of particles around 0.2-0.3 μm.

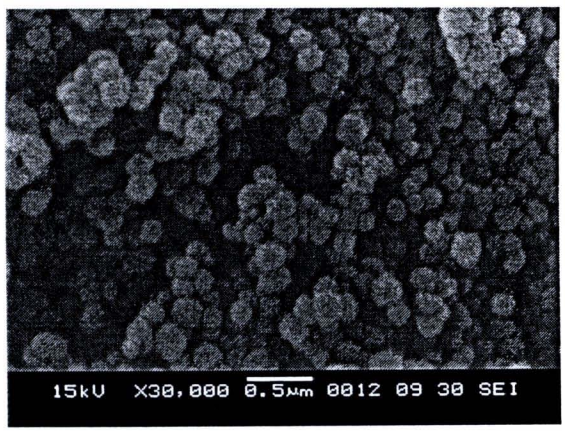

Figure 4.7 SEM image of zeolite beta (Si/Al=60).

4.1.4.2 SEM image of Al-HMS

Figure 4.8 showed the SEM images of Al-HMS with Si/Al mole ratio of 60. All synthesized materials exhibited mixed morphology between crystalline particles and amorphous materials. However, the agglomeration of small amorphous particles were mainly observed, which was in agreement with the broad XRD peak of Al-HMS. The particle size of crystalline material was ranged in 0.2-0.8 μm.

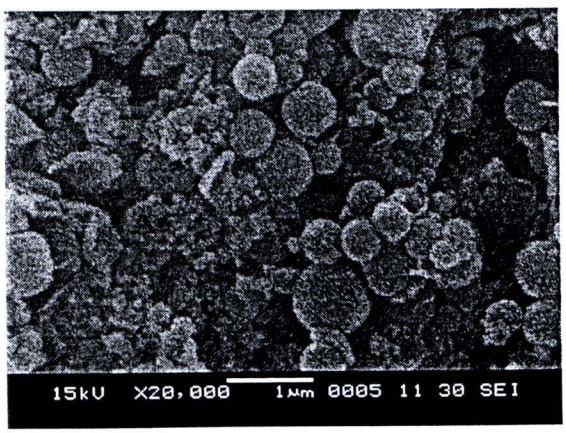

Figure 4.8 SEM images of Al-HMS (Si/Al = 60).

4.1.4.3 SEM image of zeolite beta/Al-HMS composite

Figure 4.9 showed the SEM images of zeolite beta/Al-HMS composite with various Si/Al ration in gel of zeolite beta of (40, 60, and 120). All synthesized materials had uniform structure of round particles with particle size average of 0.25-0.35 μm, which was similar to zeolite beta [61].

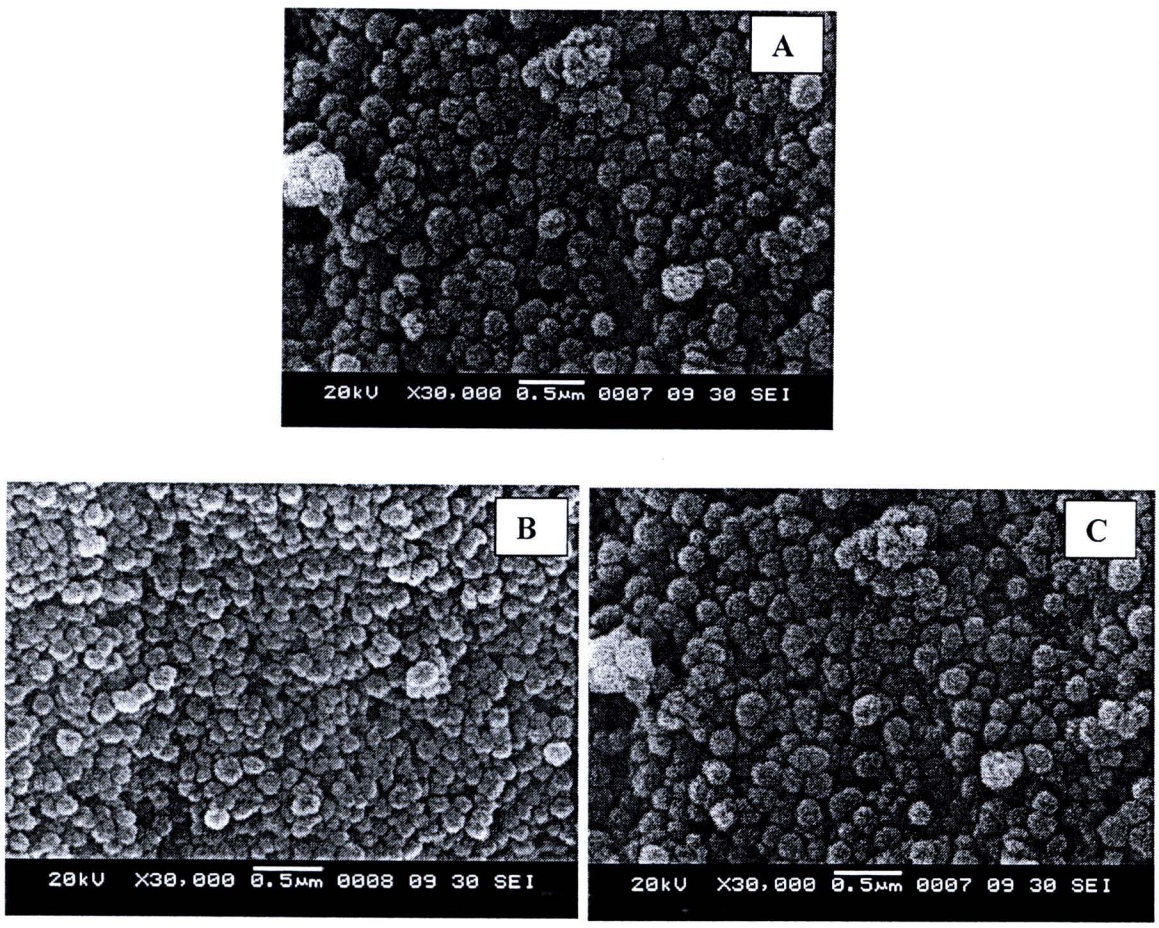

Figure 4.9 SEM images of calcined composite with various Si/Al ration in gel of zeolite beta of (a) 40, (b) 60, and (c) 120.

4.1.5 Elemental analysis

Table 4.1 showed the Si/Al mole ratio in gel and in Al-HMS, zeolite beta and zeolite beta/Al-HMS composite catalyst. The elemental analysis results suggested that the parts of aluminum were incorporated in the structure of catalyst.

Table 4.1 Physicochemical properties of the catalysts.

Samples	Si/Al mole ratio	
	In gel composition[a]	In catalysts[b]
Al-HMS	60	60.9
Zeolite beta	60	25.0
Zeolite beta/Al-HMS composite	40	23.5
Zeolite beta/Al-HMS composite	60	43.7
Zeolite beta/Al-HMS composite	120	75.0

[a]Calculated from reagent quantities;

[b]Alumimum (Al) was determined by ICP-AES

4.1.6 Nitrogen Adsorption-Desorption of catalyst

4.1.6.1 Nitrogen Adsorption-Desorption of zeolite beta

The adsorption isotherm of zeolite beta in Figure 4.10 (a) indicated type I isotherm of microporous material. A rapid increase in adsorbed volume and a plateau were found at very low P/P_0. A small increase in the adsorbed volume was observed from $P/P_0 = 0.9$, suggesting the presence of a small amount of mesopores on the surface. Pore size distribution calculated from the adsorption data by means of the MP plot method was displayed in Figure 4.10 (b). The narrow pore size distribution of the calcined zeolite beta sample was observed with the peak centered at 0.6 nm. A textural property of calcined zeolite beta sample was summarized in Table 4.2.

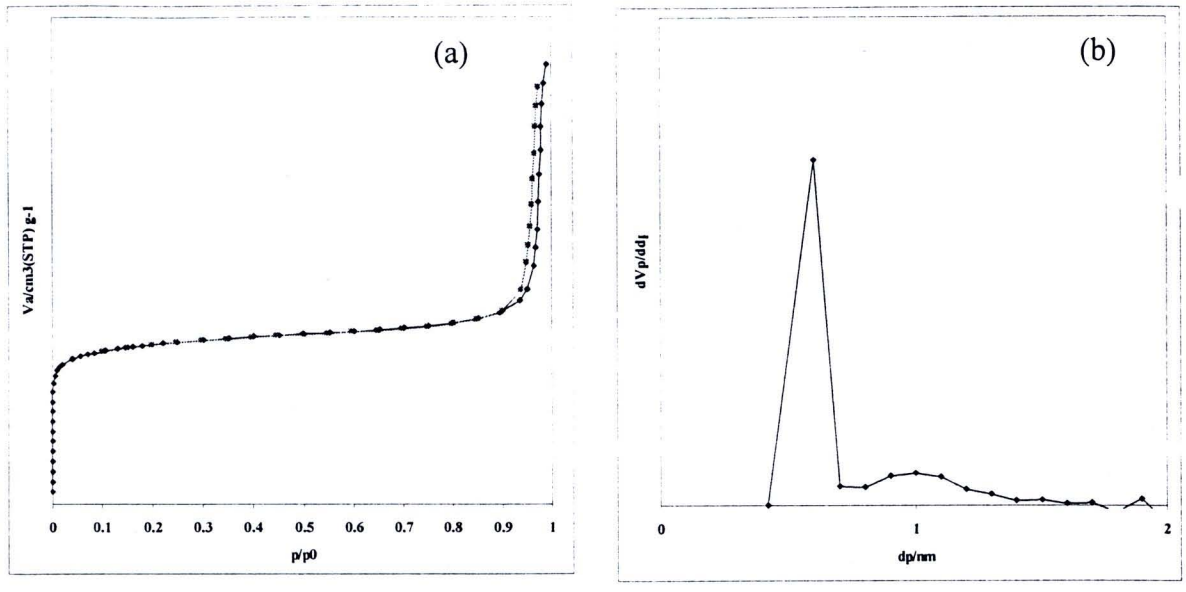

Figure 4.10 (a) N_2 adsorption-desorption isotherm (b) Pore-size distribution of zeolite beta (Si/Al=60).

4.1.6.2 Nitrogen Adsorption-Desorption of Al-HMS

The nitrogen-adsorption isotherm at 77 K of calcined Al-HMS (Si/Al=60) was illustrated in Figure 4.11(a). Calcined Al-HMS sample presented a type IV isotherm in the IUPAC classification, and typical distribution for mesoporous material.

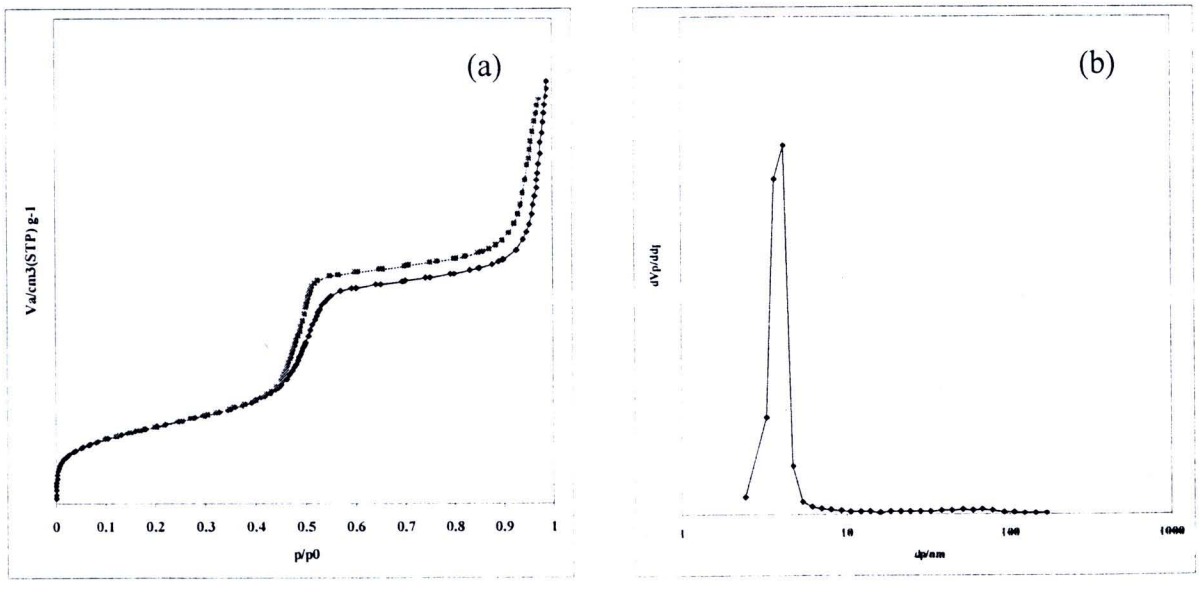

Figure 4.11 (a) N_2 adsorption-desorption isotherm (b) BJH pore-size distribution of Al-HMS (Si/Al =60).

Pore size distribution was calculated from the adsorption data by means of the Barrett, Joyner and Halenda (BJH) method and was shown in Figure 4.11(b). The pore size distribution of Al-HMS (Si/Al = 60) was approximately 4.2 nm. Textural properties of Al-HMS were also displayed in Table 4.2.

Table 4.2 Textural properties of calcined zeolite beta and Al-HMS samples.

Samples	Si/Al mole ratio in gel[a]	Si/Al mole ratio in product[b]	BET specific surface (m^2/g)	Pore volume (cm^3/g)	Pore diameter (nm)
Zeolite beta	60	25	737	0.3	0.6
Al-HMS	60	60.9	843	2.1	4.2

a: Calculated from reagent quantities.

b: Aluminum (Al) was determined by ICP-AES and Si was calculated from the deduction of AlO_2 from the sample weight.

4.1.6.3 Nitrogen Adsorption-Desorption of zeolite beta/Al-HMS composite

4.1.6.3.1 Effect of NaOH concentration and time on dissolving zeolite beta

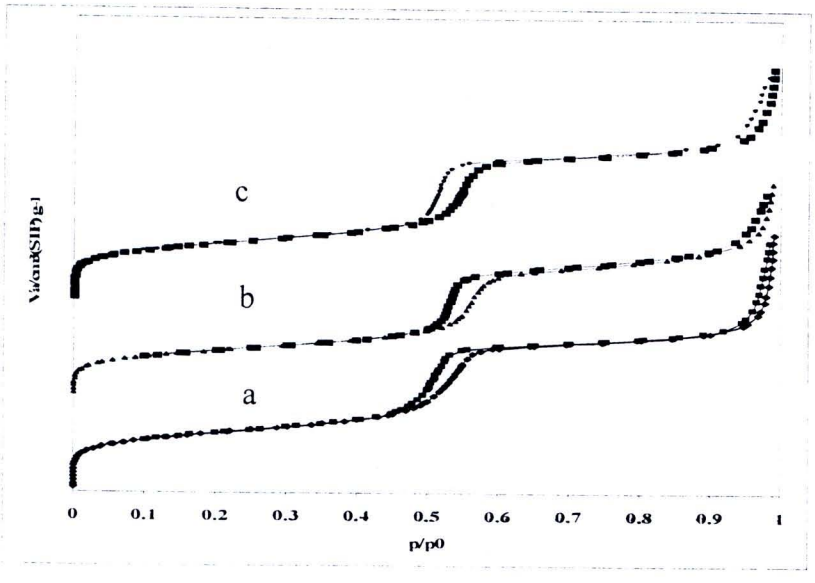

Figure 4.12 Adsorption and desorption isotherms of composites with (a) 1 M NaOH 15 min (b) 1 M NaOH 30 min (c) 0.5 M NaOH 30 min.

The N_2 adsorption-desorption isotherms of the calcined zeolite beta/Al-HMS composites with various concentrations of NaOH and time on dissolution of zeolite beta were shown in Figure 4.12. All samples gave a typical isotherm of type IV. Each isotherm exhibited three stages as follows: at low pressure (P/Po < 0.3) the adsorption was accounted by a monolayer adsorption of nitrogen on the walls of mesopore. As the relative pressure increased (P/Po = 0.3-0.5), a steep rise in capillary condensation was observed within mesopores. At higher relative pressure (P/Po > 0.5), the plateau region was due to the fully pore filling followed by multilayer adsorption on the surface of the particles. The specific BET surface area of samples calculated from the adsorption data were 671, 382, and 664 m^2/g for 1 M NaOH 15 min, 1 M NaOH 30 min, and 0.5 M NaOH 30 min, respectively.

4.1.6.3.2 Effect of Si/Al ratio

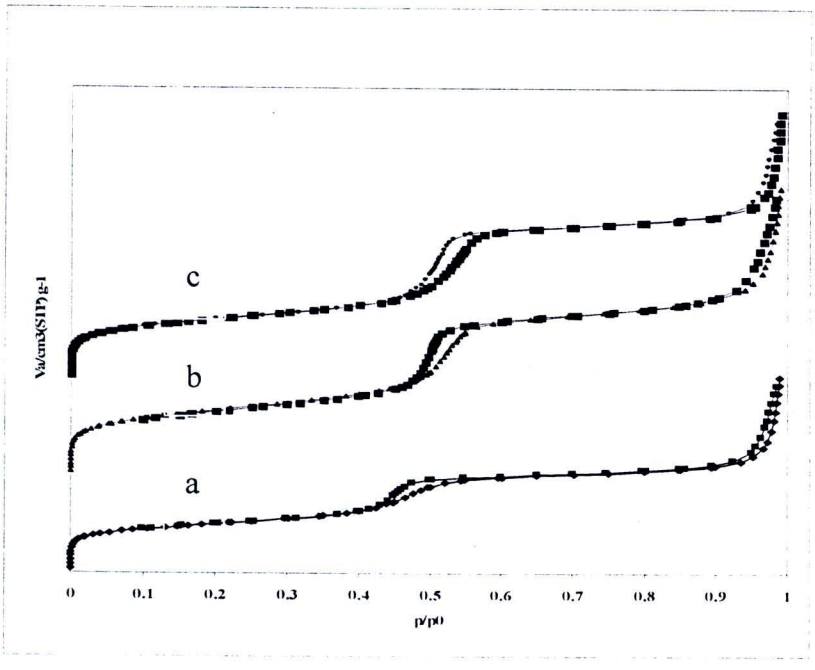

Figure 4.13 Adsorption and desorption isotherms of composite with various Si/Al ration in gel of zeolite beta of (a) 40, (b) 60, and (c) 120.

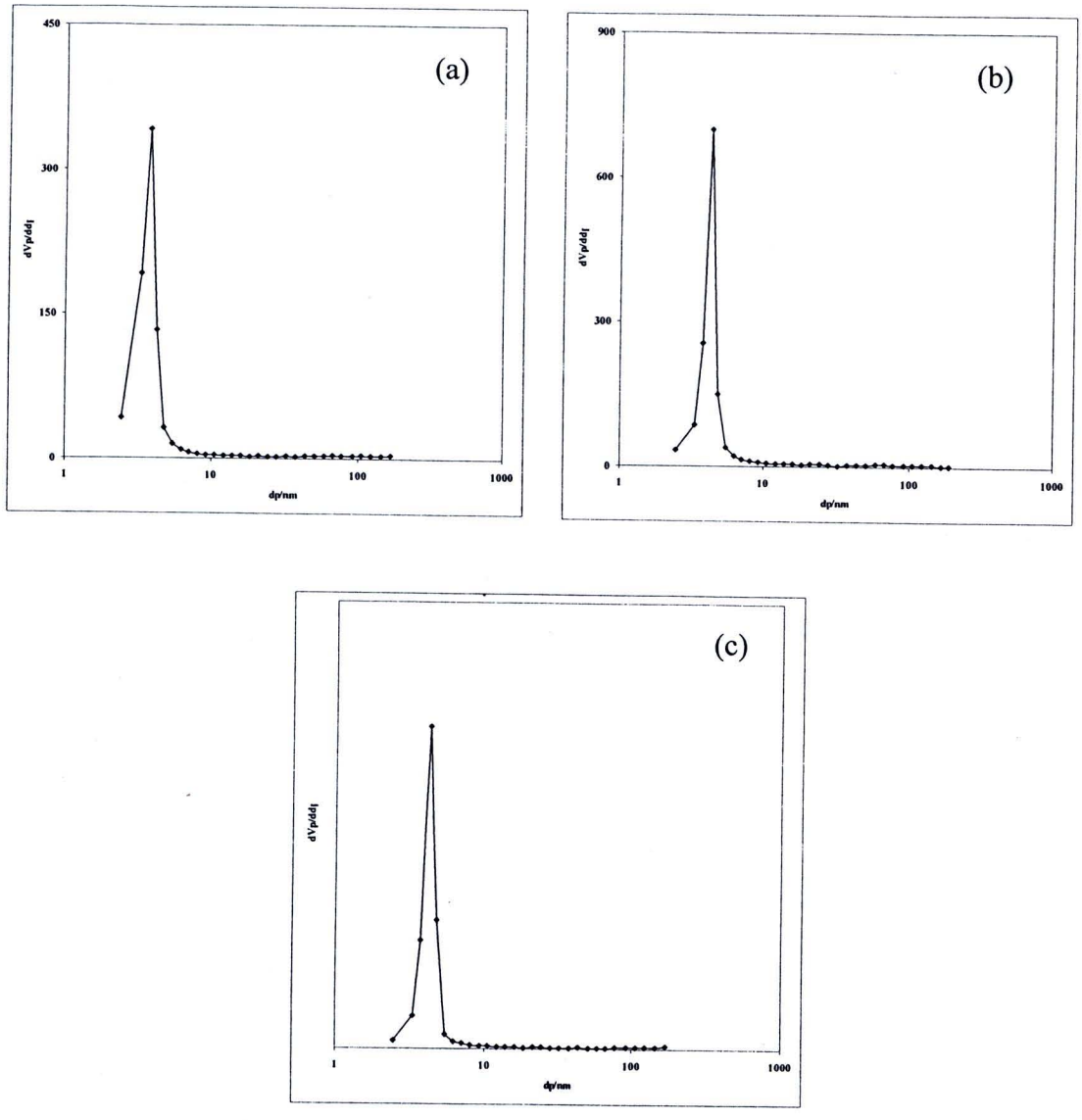

Figure 4.14 BJH pore size distribution of composites with various Si/Al ration in gel of zeolite beta of (a) 40, (b) 60, and (c) 120.

Zeolite beta/Al-HMS composites with various Si/Al ration in gel of zeolite beta were synthesized using 1 M NaOH as a dissolving solution for 15 min and crystallization time of 36 h. N_2 adsorption-desorption isotherms of all calcined composites gave a typical isotherm of type IV, as shown in Figure 4.16. The specific BET surface areas were 538, 724, and 671 m^2/g for composites with Si/Al ration in zeolite beta of 40, 60, and 120, respectively. The BJH pore size distributions were 3.71, 4.19 and 4.19 nm for composites with Si/Al ration in zeolite beta of 40, 60, and 120, respectively.

4.1.7 ^{27}Al-MAS-NMR Spectrum

4.1.7.1 ^{27}Al-MAS-NMR Spectrum of zeolite beta

The ^{27}Al-MAS-NMR spectra of calcined zeolite beta were displayed in Figure 4.15. The signal at 53 ppm was typically assigned to tetrahedrally coordinated (T_d) framework aluminum, and the peak at 0 ppm was assigned to the octahedrally coordinated (O_h) non-framework aluminum [62]. Zeolite beta showed two peaks at the chemical shift around 53 ppm, which was the tetrahedral aluminum in the framework position, and 0 ppm which was octahedral, respectively.

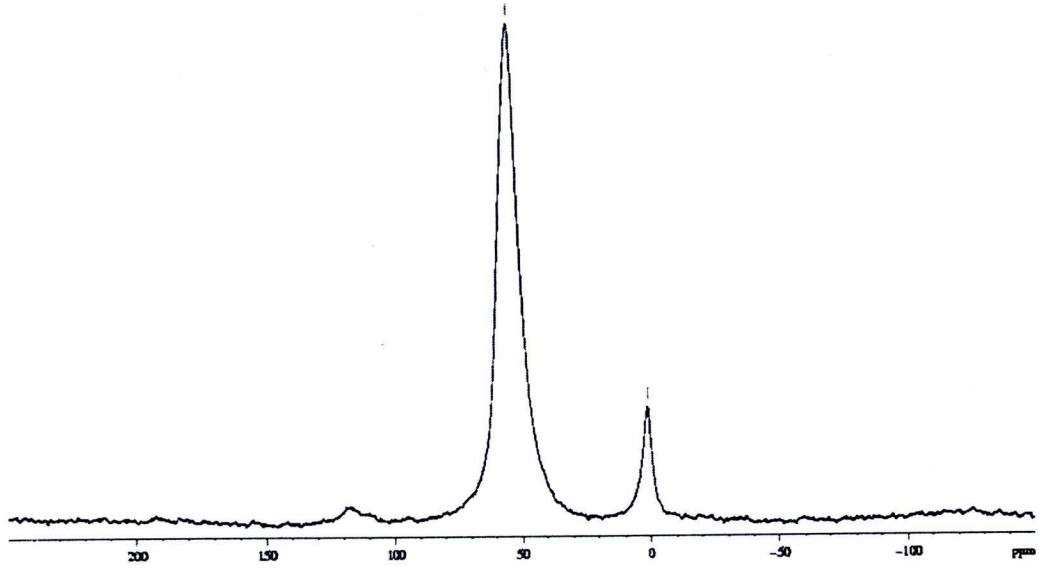

Figure 4.15 ^{27}Al-MAS-NMR spectrum of calcined zeolite beta.

4.1.7.2 ^{27}Al-MAS-NMR Spectrum of Al-HMS

Figure 4.16 showed the ^{27}Al-MAS-NMR spectrum of calcined Al-HMS with Si/Al ratio of 60. The spectrum of calcined sample showed two signal peaks of octahedral and tetrahedral coordination.

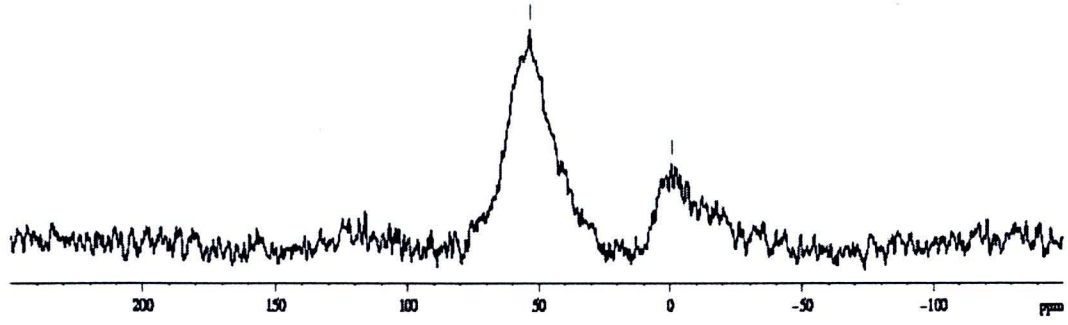

Figure 4.16 ^{27}Al-MAS-NMR spectrum of calcined Al-HMS with Si/Al (60).

4.1.7.3 ^{27}Al-MAS-NMR Spectrum of zeolite beta/Al-HMS composite

^{27}Al-MAS-NMR spectra of calcined composite samples with different Si/Al ration in gel of zeolite beta were displayed in Figure 4.17. All samples showed the presence of an intense signal centered at 55 ppm which corresponded to aluminum in tetrahedral (T_d) framework position [62]. No octahedral coordination was observed. The data indicated all Al atoms in the composite were incorporated in the tetrahedrally coordinated (T_d) framework silica.

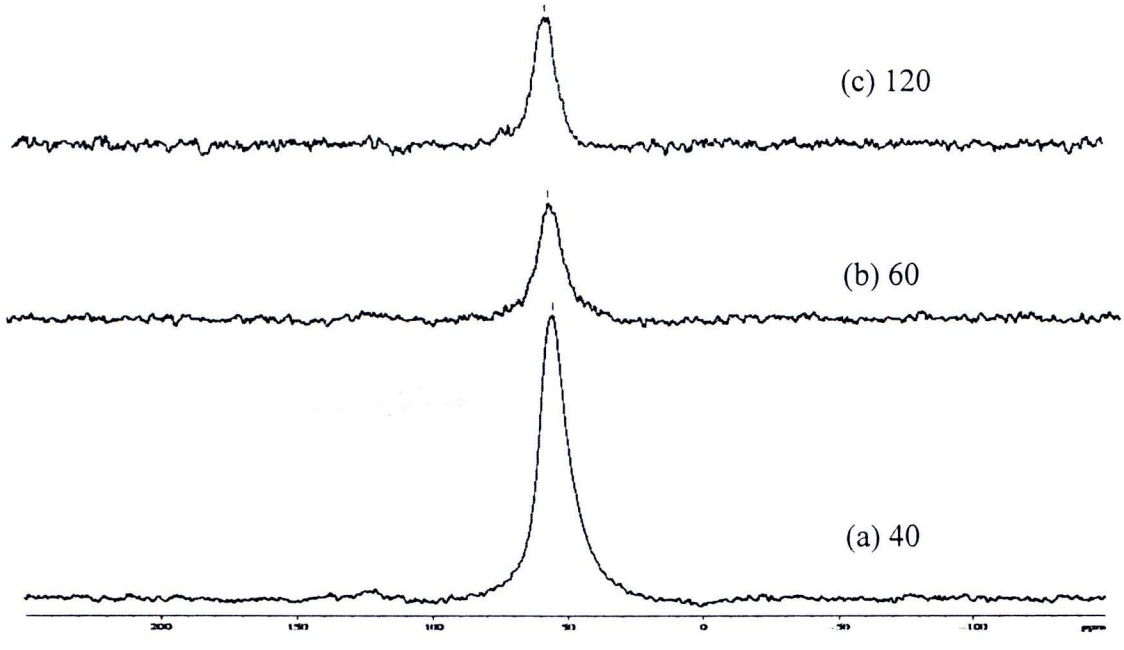

Figure 4.17 ^{27}Al-MAS-NMR spectra of calcined composites with different Si/Al ration in zeolite beta of (a) 40, (b) 60, and (c) 120.

4.2 Catalytic activity test

4.2.1 Conversion of lubricant oil

4.2.1.1 Effect of the reaction time

Cracking of lubricant oil over zeolite beta/Al-HMS composite catalyst with Si/Al ratio in gel of zeolite beta of 60 was carried out at 400°C for 120 min. Figure 4.18 illustrated the accumulative volume of liquid fraction in the reaction. It was found that when the reaction time was increased, the accumulative volume was increased and after 90 min the total accumulative liquid volume was not much changed. In order to find optimal reaction time for lubricant oil cracking, the reaction time for 90 and 120 min were compared, the cracking results were summarized in Table 4.3. By increasing the reaction time, the value of %conversion was increased. Moderate conversion of lubricant oil into products was observed and resulted in liquid and gas products. When reaction time was increased, zeolite beta/Al-HMS composite catalyst facilitated the cracking of lubricant oil into low molecular weight molecules, resulting dramatically increase in gas yield. The liquid yield consisted of a fraction of light hydrocarbons, which continued cracking until it became lighter molecules or gaseous product. In this work the yield of distillate oil was considered, the yields of distillate oil over the composite catalyst were calculated as 5.11 and 4.34 for the reaction time of 90 and 120 min, respectively. From these results, the reaction time for 90 min was chosen for further study due to providing the high value of distillate oil.

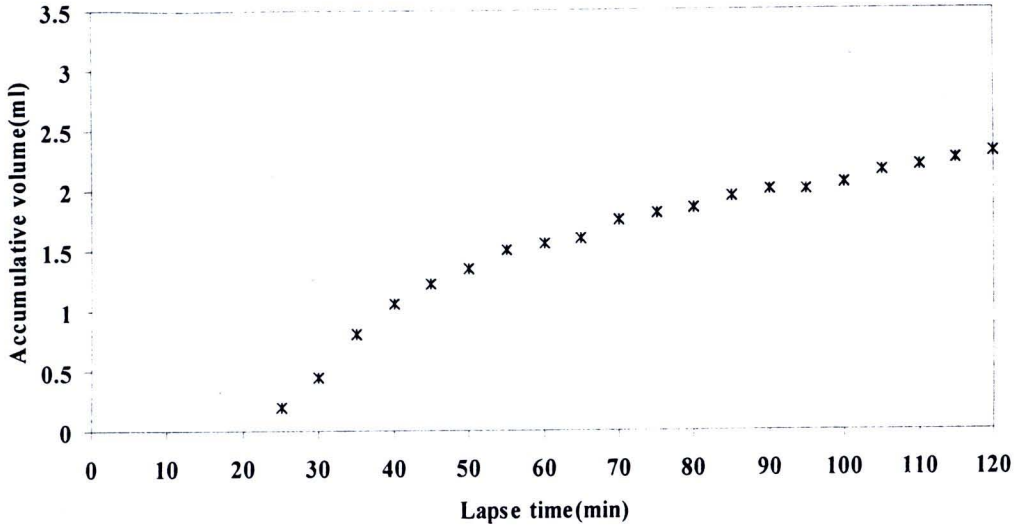

Figure 4.18 Accumulative volume of liquid fractions from catalytic cracking of lubricant oil over zeolite beta/Al-HMS composite catalysts at 400°C for 120 min.

Table 4.3 Catalytic cracking of lubricant oil over zeolite/Al-HMS composite catalyst at 400°C

Reaction time	90 min	120 min
	Zeolite beta/Al-HMS	Zeolite beta/Al-HMS
%Conversion*	65.4	77.0
%Yield* 1. gas fraction	32.8	40.2
2. liquid fraction	32.6	36.8
3. residue	34.6	23.0
%Selectivity of liquid fraction		
1. distillate oil (%yield of distillate oil)**	15.7 (5.11)	11.8 (4.34)
2. heavy oil	84.3	88.2
Liquid fraction density (g/cm^3)	0.81	0.80

Condition: N_2 flow of 20 cm^3/min, the reaction temperature of 400°C, 10wt% catalyst to lubricant oil. *Deviation within ±1.1% for conversion, ±0.6% for yield of gas fraction, ±0.9% for yield of liquid fraction, and ±1.0% for yield of residue. **%yield of distillate oil = %yield of liquid fraction × %selectivity of liquid fraction and divided by 100.

4.2.1.2 Effect of the reaction temperatures

Table 4.4 summarized the values of %conversion and %yield obtained by thermal cracking and catalytic cracking of lubricant oil over zeolite beta/Al-HMS composite catalyst with Si/Al ratio in gel of zeolite beta of 60 at the reaction temperatures of 350, 380 and 400°C for 90 min. The value of %conversion was increased and could be observed from gas and liquid fraction when the reaction temperatures were increased, suggesting that the reaction temperatures promoted the cracking reaction via carbocation and free radicals mechanism.

Considering between thermal cracking and catalytic cracking, it was found that at the reaction temperature below 380°C, catalytic cracking showed higher conversion than thermal cracking due to the acidity of the catalyst. However, thermal effect played an important role in cracking reaction at the high reaction temperature. The value of %conversion over zeolite beta/Al-HMS composite catalyst increased from 11.2% to 65.4% when reaction temperature was increased from 350°C to 400°C.

Table 4.4 Thermal and catalytic cracking of lubricant oil over zeolite/Al-HMS composite catalyst at various the reaction temperatures for 90 min

	Reaction temperatures					
	350°C		380°C		400°C	
	Thermal	zeolite beta/AlHMS	Thermal	zeolite beta/AlHMS	Thermal	zeolite beta/AlHMS
%Conversion*	7.8	11.2	37.2	61.6	74.6	65.4
%yield* 1. gas fraction	5.2	7.2	13.0	28.8	31.2	32.8
2. liquid fraction	2.6	4.0	24.2	32.8	43.4	32.6
3. residue	92.2	88.8	62.8	38.4	25.4	34.6
%selectivity of liquid fraction						
1. distillate oil (%yield of distillate oil)**	-	-	4.0 (0.96)	17.2 (5.64)	10.7 (4.64)	15.7 (5.11)
2. heavy oil	-	-	96.0	82.8	89.3	84.3
Liquid fraction density (g/cm^3)	-	-	1.30	1.30	0.81	0.81

Condition: N_2 flow of 20 cm^3/min, the reaction time of 90 min, 10wt% catalyst to lubricant oil. *Deviation within ±1.0% for conversion, ±0.5% for yield of gas fraction, ±0.9% for yield of liquid fraction, and ±0.9% for yield of residue. **%yield of distillate oil = %yield of liquid fraction × %selectivity of liquid fraction and divided by 100.

The liquid yield was slightly changed after 380°C, whereas the yield of distillate oil at 380°C was greater than the others. From this result, it was suggested that the catalytic cracking showed the highest efficiency to produce the yield of distille oil in cracking of lubricant oil at 380°C. Then, the reaction temperature of 380°C was selected to be the best test condition for further studies in this work.

Figure 4.19 showed distribution of gas fraction obtained by catalytic cracking of lubricant oil over zeolite beta/Al-HMS composite at 350°C, 380°C and 400°C. The compositions of gas fraction were similar and mainly composed of 1,3-butadiene, propene, ethane, i-butene and acetylene. When the reaction temperature was increased, the gas fractions of lighter hydrocarbon (methane, ethane and propene) were increased, while those of heavier hydrocarbons ($C5^{+}$) were decreased. The growing yield of volatile components as function of the reaction temperature could be caused by the differences in thermal stability of hydrocarbon chain. At higher reaction temperatures, hydrocarbon chain had low thermal stability resulting that C-C bonds easily break into short-chain hydrocarbon.

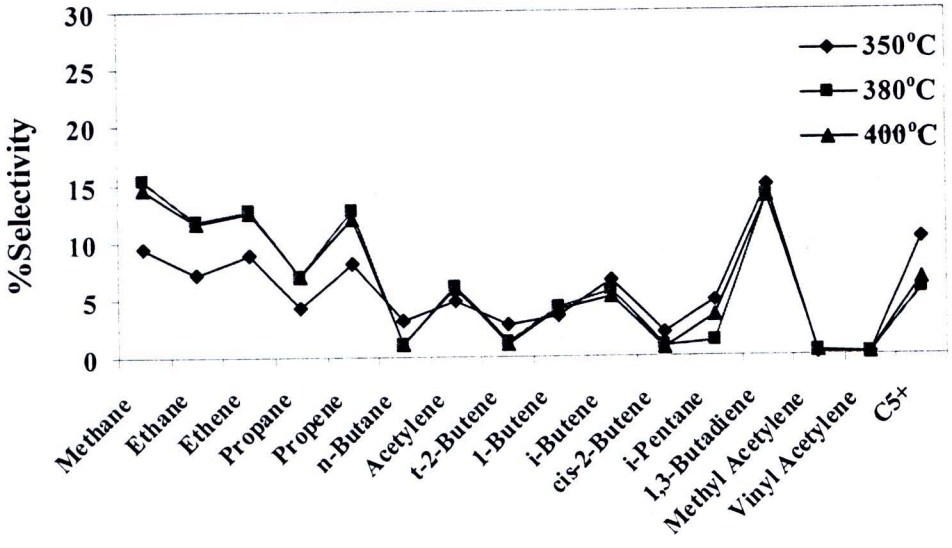

Figure 4.19 Distribution of gas fraction obtained by catalytic cracking of lubricant oil over zeolite beta/Al-HMS composite catalyst at various the reaction temperatures for 90 min.

4.2.1.3 Effect of various catalysts

Thermal cracking and catalytic cracking of lubricant oil over Al-HMS, zeolite beta, zeolite beta/Al-HMS composite catalysts were compared at 380°C for 90 min. The values of %conversion and %yields were shown in Table 4.5. The value of %conversion and %yield of liquid fraction over zeolite beta/Al-HMS composite catalyst was slightly higher than zeolite beta, whereas gas fraction was not different. This result indicated that the acidity of zeolite beta/Al-HMS composite less than zeolite beta resultd in the liquid product that archived by composite catalyst was slightly higher. In addition, pore size of zeolite beta/Al-HMS composite was slightly larger than zeolite beta then large molecules can access pore better than zeolilte beta and produce large molecule product (heavy oil) more than the zeolite beta catalyst. Besides, the yield of distillate oil between composite and zeolite beta were also similar.

On the other hand, the gas fraction and liquid fraction of zeolite beta/Al-HMS composite catalyst were higher than Al-HMS. These results were also explained by the acidity of composite was higher than Al-HMS, then aluminum content in catalyst accelerated the degradation of hydrocarbon chain proceeding through carbocation mechanism. Comparison of the selectivity and yield of distillate oil between the zeolite beta/Al-HMS composite and Al-HMS catalysts, the composite catalyst gave the selectivity and yield of distillate oil more than Al-HMS catalyst because the zeolite beta/Al-HMS composite had small pore, which enhanced small molecules to enter pore and gave high distillate oil.

Table 4.5 Thermal and catalytic cracking of lubricant oil over Al-HMS, zeolite and zeolite/Al-HMS composite catalyst at 380°C for 90 min.

	Reaction temperature at 380°C			
	Thermal	**Al-HMS**	**Zeolite beta**	**zeolite beta/AlHMS**
%Conversion*	37.2	41.8	57.0	61.6
%yield* 1. gas fraction	13.0	16.6	30.4	28.8
2. liquid fraction	24.2	25.2	26.6	32.8
3. residue	62.8	58.2	43.0	38.4
%selectivity of liquid fraction				
1. distillate oil (%yield of distillate oil)**	4.0 (0.96)	8.2 (2.06)	20.0 (5.32)	17.2 (5.64)
2. heavy oil	96.0	91.8	80.0	82.8
Liquid fraction density (g/cm^3)	0.96	0.96	0.86	0.86

Condition: N_2 flow of 20 cm^3/min, the reaction temperature of 380°C for 90 min, 10wt% of catalyst to lubricant oil. *Deviation within ±1.0% for conversion, ±0.5% for yield of gas fraction, ±0.9% for yield of liquid fraction, and ±0.9% for yield of residue. **%yield of distillate oil = %yield of liquid fraction × %selectivity of liquid fraction and divided by 100.

The composition of gaseous products from lubricant oil cracking at 380°C was shown in Figure 4.20. The gas fraction obtained by thermal cracking consisted of ethane, propene, i-butene, 1,3-butadiene, and $C5^+$. For catalytic cracking, the gas components obtained from cracking of the composite catalyst were similar to those of Al-HMS catalyst. The major components were methane, ethane, propene, 1,3-butadiene, and $C5^+$. Whereas, gas components obtained from zeolite beta catalyst were different from those catalysts, the main components were n-butane, i-pentane, 1,3-butadiene and C_5^+.

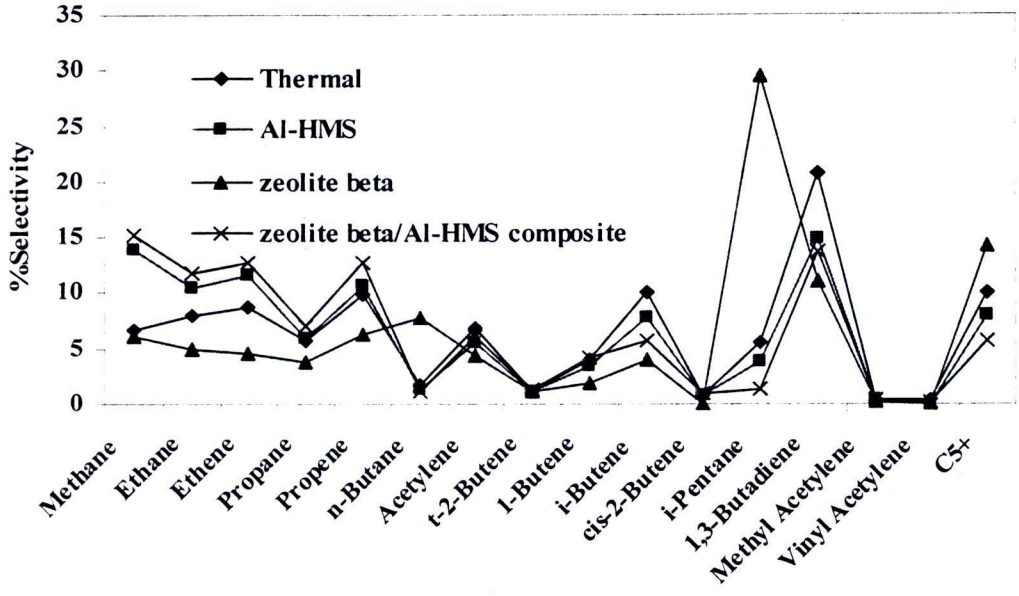

Figure 4.20 Distribution of gas fraction obtained by thermal and catalytic crackings of lubricant oil over Al-HMS, zeolite beta and zeolite beta/Al-HMS composite catalysts at 380°C for 90 min.

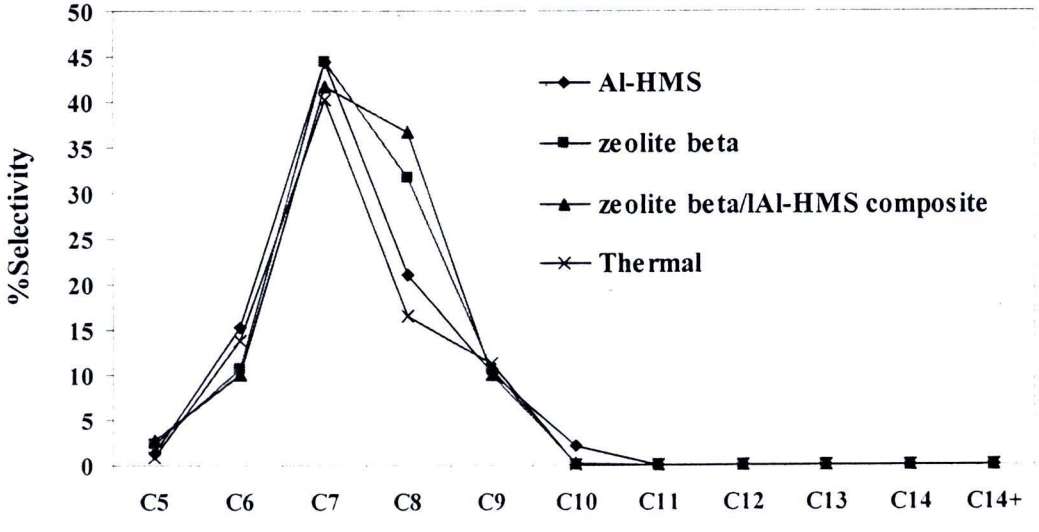

Figure 4.21 Carbon number distribution of distillate oil obtained by thermal and catalytic crackings of lubricant oil over Al-HMS, zeolite beta and zeolite beta/Al-HMS composite catalysts at 380°C for 90 min.

Figure 4.20 showed the product distribution of distillate oil obtained by thermal cracking and catalytic cracking of lubricant oil over zeolite beta/Al-HMS composite at 380°C for 90 min. All liquid products were mainly distributed in the

hydrocarbon range of C_6-C_{10}. The liquid products of the composite and zeolite beta catalysts were enriched in C_7-C_8, while those of others were mainly in C_7.

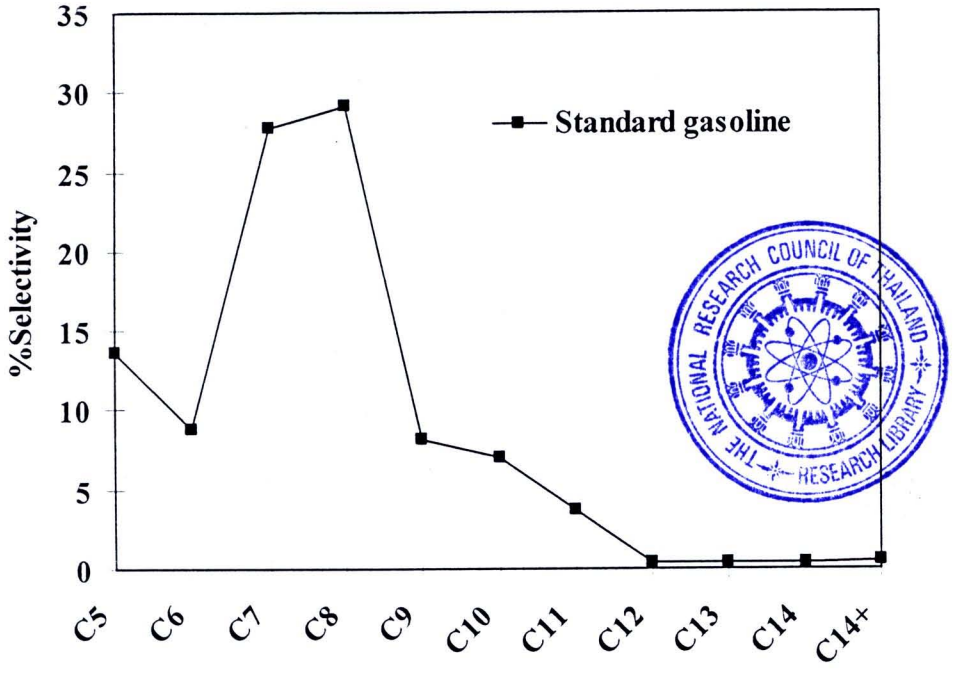

Figure 4.22 Carbon number distribution of commercial SUPELCO standard gasoline fraction.

The product distribution of SUPELCO standard gasoline fraction was shown in Figure 4.22. The major components were C_7 and C_8, based on the boiling point range using n-paraffins as reference. %Selectivity of standard gasoline was calculated following the appendice, the concentration of each fraction from certificated report divided by the total concentration of the fractions and multiplied by 100. When the liquid distribution of composite catalyst was compared to the SUPLECO standard, it was observed that liquid products obtained from cracking of lubricant oil over composite material gave the similar hydrocarbon number as the SUPLECO standard distribution.

4.2.2 Conversion of grease

4.2.2.1 Effect of the reaction temperatures

The %conversion and %yield from thermal and catalytic crackings of grease over zeolite beta/Al-HMS composite catalyst with Si/Al ratio of 60 in gel of zeolite beta with various reaction temperatures of 350, 380 and 400°C were shown in Table 4.6. The reaction time was fixed at 90 min based on the condition of lubricant oil in section 4.2.1.1. The %selectivity to gas and liquid products were increased when the reaction temperatures were increased because the high reaction temperatures promoted the cracking reaction via carbocation and free radicals mechanisms. However, the %conversion was minimal at 350°C and showed the least active.

Comparing between thermal and catalytic crackings at the same reaction temperature, it was found that catalytic cracking showed higher %conversion than thermal cracking because the acidity of catalyst promoted the degradation of grease via carbocation mechanism [55-58]. The conversion value of zeolite beta/Al-HMS composite increased from 4.8% to 67% when the reaction temperature was raised from 350°C to 400°C.

Furthermore, the liquid yield at 400°C was higher than 350°C and 380°C. The selectivity and yield of distillate oil were occurred at the reaction temperature of 400°C only. Additionally, catalytic cracking exhibited higher the selectivity and yield of distillate oil than thermal cracking. From this result, the composite catalyst showed the highest efficiency in cracking of grease at 400°C. Therefore, the reaction temperature at 400□C was the optimized condition in this work.

Figure 4.23 showed distribution of gas fraction obtained by catalytic cracking of grease over zeolite beta/Al-HMS composite at 350°C, 380°C and 400°C. The major components were 1,3-butadiene, propene and acetylene. When the reaction temperature was increased, the gas fractions of lighter hydrocarbon (methane and ethene) were increased, while those of heavier hydrocarbons (1,3-butadiene and C_5^+) were decreased. The growing yield of volatile components as function of temperature could be caused by the differences in the thermal stability of hydrocarbon chain. At high temperature, hydrocarbon chain had low thermal stability then C-C bonds easily break into short-chain hydrocarbon.

Table 4.6 Thermal and catalytic cracking of grease over zeolite/Al-HMS composite catalyst at various temperatures for 90 min

	Reaction temperatures					
	350°C		380°C		400°C	
	Thermal	zeolite beta/AlHMS	Thermal	zeolite beta/AlHMS	Thermal	zeolite beta/AlHMS
%Conversion*	4.6	4.8	10.2	18.2	35.0	67.0
%yield* 1. gas fraction	2.2	2.8	4.0	10.4	17.2	29.2
2. liquid fraction	2.4	2.0	6.2	7.8	17.8	37.8
3. residue	95.4	95.2	66.4	81.8	9.4	3.6
%selectivity of liquid fraction						
1. distillate oil (%yield of distillate oil)**	-	-	-	-	12.8 (2.28)	22.2 (8.39)
2. heavy oil	-	-	-	-	87.2	33.0
Liquid fraction density (g/ cm^3)	-	-	0.13	1.30	0.83	0.77

Condition: N_2 flow of 20 cm^3/min, the reaction time of 90 min, 10 wt% of catalyst to grease. *Deviation within ±1.1% for conversion, ±0.6% for yield of gas fraction, ±1.0% for yield of liquid fraction, and ±0.9% for yield of residue. **%yield of distillate oil = %yield of liquid fraction × %selectivity of liquid fraction and divided by 100.

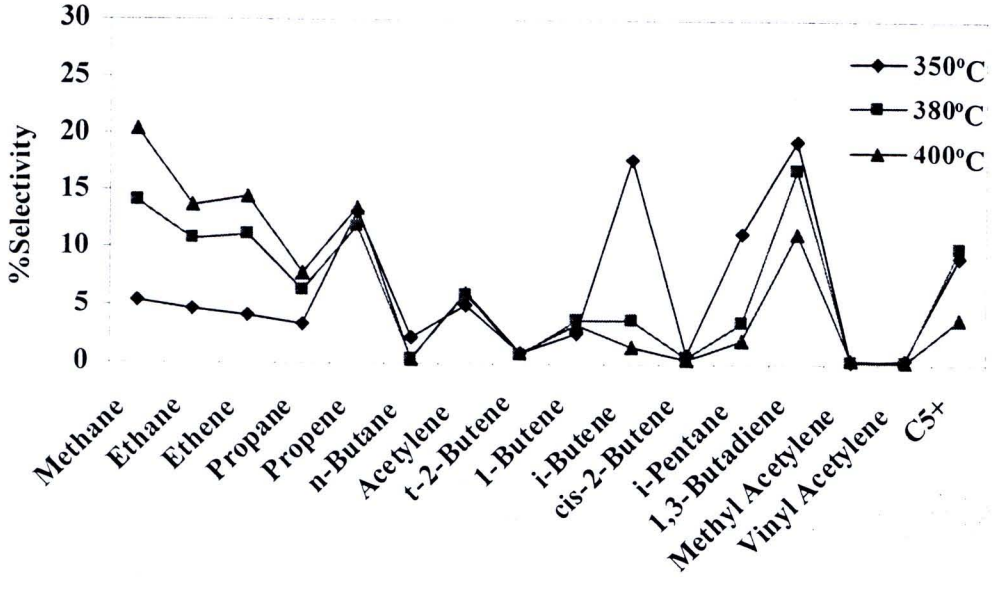

Figure 4.23 Distribution of gas fraction obtained by catalytic cracking of grease over zeolite beta/Al-HMS composite catalyst at various the reaction temperature.

4.2.2.2 Effect of the reaction time

Cracking of grease over zeolite beta/Al-HMS composite catalyst with Si/Al ratio in gel of zeolite beta of 60 was studied at 400°C for 120 min. Figure 4.24 showed the accumulative volume of liquid fractions in the reaction. It was found that the accumulative volume increased when the reaction time increased. However, the initial rate of liquid fraction formation in the catalytic cracking was much faster than thermal cracking, indicating the predominant competition of composite catalyst in dissociation of grease into liquid formation. It was noticed that the total accumulative liquid volume seemed to be constant after 90 min. In order to find the optimal reaction time for grease cracking, the reaction times at 90 and 120 min were considered. The data was summarized in Table 4.7. By increasing the reaction time, %conversion was increased. A high conversion of grease into products was observed and resulted in the increase in yields of liquid and gas products whereas the residue yield was decreased. It was suggested that zeolite beta/Al-HMS composite catalyst facilitated the cracking of grease into low molecular weight molecules. When the reaction time was increased, grease had more time to react with the catalyst and produced more liquid and gas products until it seem to be constant.

Moreover, the selectivity to distillate oil at 90 and 120 min were not different. Nevertheless, the yields of distillate oil were 8.39 and 9.57 at the reaction time of 90 and 120min, respectively. From this result, the composite catalyst showed the highest conversion and liquid fraction in cracking of grease at the reaction time of 120 min. Therefore, the reaction time for 120 min at 400°C was chosen for further study in this research.

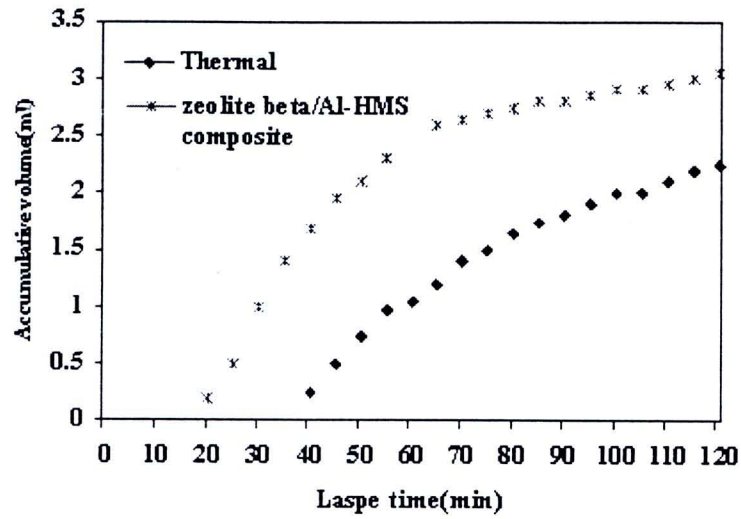

Figure 4.24 Accumulative volume of liquid fractions from thermal and catalytic crackings of grease over zeolite beta/Al-HMS composite catalyst at 400°C for 120 min.

Table 4.7 Catalytic cracking of grease over zeolite/Al-HMS composite catalyst at the reaction temperature of 400°C

Reaction time	90 min	120 min
	Zeolite beta/Al-HMS	Zeolite beta/Al-HMS
%Conversion*	67.0	82.2
%Yield* 1. gas fraction	29.2	34.8
2. liquid fraction	37.8	47.4
3. residue	33.0	17.8
%Selectivity of liquid fraction		
1. distillate oil (%yield of distillate oil)**	22.2 (8.39)	20.2 (9.58)
2. heavy oil	77.8	79.8
Liquid fraction density (g/ cm^3)	0.78	0.77

Condition: N_2 flow of 20 cm^3/min, the reaction temperature of 400°C, 10wt% of catalyst to grease. *Deviation within ±1.0% for conversion, ±0.5% for yield of gas fraction, ±0.9% for yield of liquid fraction, and ±0.9% for yield of residue. **%yield of distillate oil = %yield of liquid fraction × %selectivity of liquid fraction and divided by 100.

4.2.2.3 Effect of various catalysts

Cracking of grease over various catalysts: Al-HMS, zeolite beta and zeolite beta/Al-HMS composite were carried out at 400oC for 120 min, the thermal cracking without catalyst was tested in comparison. These result showed in Table 4.8.

Conversion and liquid fraction of zeolite beta/Al-HMS composite was higher than zeolite beta. The result indicated that pore size of zeolite beta/Al-HMS composite was larger than zeolite beta resulting that the large molecule can access pore better than zeolilte beta then conversion was greater in liquid yield. In addition, the acidity of zeolite beta/Al-HMS composite was less than zeolite beta confirming with ICP-AES and ^{27}Al-MAS-NMR techniques. Likewise, the selectivity and yield of distillate oil of composite were higher than zeolite beta. These results could be explained by various pore sizes of composite catalyst. The large pore size of composite allowed large molecules to access the pore and broke the long hydrocarbon chain from ends into small unit or oligomer. Then these oligomers diffused into small pore or channel of composite and broke into smaller molecules [54]. It was also confirmed by accumulative volumes of liquids obtained over various catalysts, which are displayed in Figure 4.25. In addition, the rate of composite material was much faster than zeolite beta.

On the other hand, the conversion of zeolite beta/Al-HMS composite catalyst was similar to Al-HMS. However, the zeolite beta/Al-HMS composite gave higher liquid fraction, selectivity and yield of distillate oil than Al-HMS catalyst because the zeolite beta/Al-HMS composite catalyst had small pore, which enhanced small molecules to enter pore and gave high distillate oil.

Table 4.8 Thermal and catalytic cracking of grease over Al-HMS, zeolite beta and zeolite/Al-HMS composite catalyst at 400°C for 120 min

	Reaction temperature at 400°C			
	Thermal	**Al-HMS**	**Zeolite beta**	**zeolite beta/AlHMS**
%Conversion*	4.0	83.0	77.6	82.2
%yield* 1. gas fraction	36.6	43.6	41.8	34.8
2. liquid fraction	37.4	39.4	35.8	47.4
3. residue	26.0	17.0	22.4	17.8
%selectivity of liquid fraction				
1. distillate oil (%yield of distillate oil)**	10.9 (4.09)	12.8 (5.03)	11.8 (4.23)	20.2 (9.58)
2. heavy oil	89.1	87.2	88.2	79.8
Liquid fraction density (g/cm^3)	0.83	0.85	0.85	0.77

Condition: N_2 flow of 20 cm^3/min, reaction temperature of 400°C for 120 min, 10wt% of catalyst to grease. *Deviation within ±1.1% for conversion, ±0.6% for yield of gas fraction, ±1.0% for yield of liquid fraction, and ±0.9% for yield of residue. *%yield of distillate oil = %yield of liquid fraction × %selectivity of liquid fraction and divided by 100.

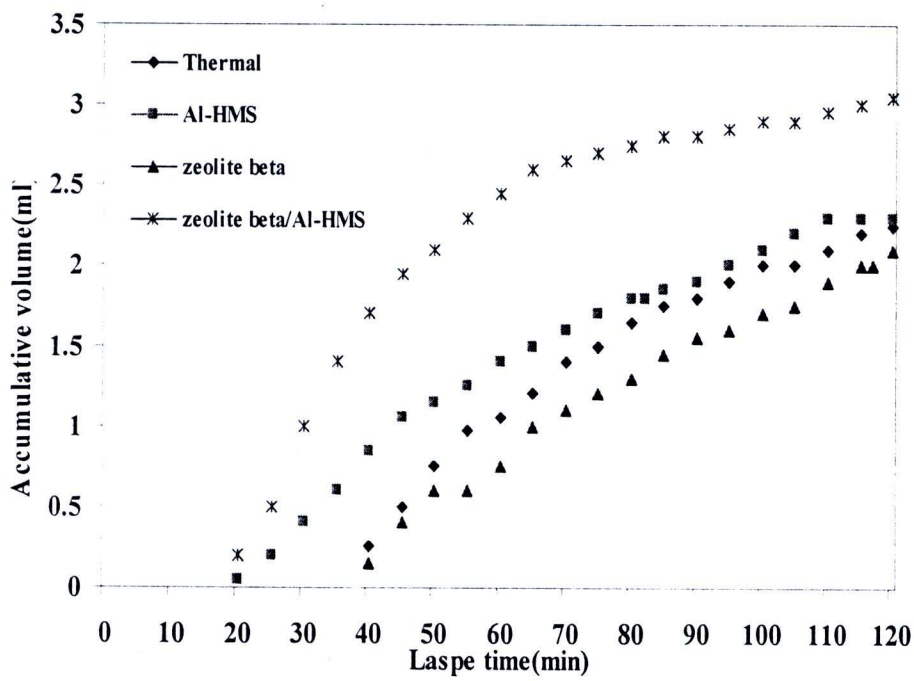

Figure 4.25 Accumulative volume of liquid fractions from thermal and catalytic cracking of grease over Al-HMS, zeolite beta and zeolite beta/Al-HMS composite catalysts at 400°C for 120 min.

The composition of gaseous products from grease cracking at 400°C for 120 min was shown in Figure 4.26. The gas fraction obtained by thermal cracking consisted of 1,3-butadiene, propene, acetylene and $C5^+$. For catalytic cracking, the gas components obtained from cracking of composite catalyst were similar to those of Al-HMS and zeolite beta catalyst. The major components were methane, ethene, propene, 1,3-butadiene and $C5^+$. The difference in gas components between thermal and catalytic crackings was explained by the different cracking mechanism. Thermal cracking proceeded through random scission via free radical mechanism, whereas catalytic cracking proceeded through carbocation mechanism [58, 59].

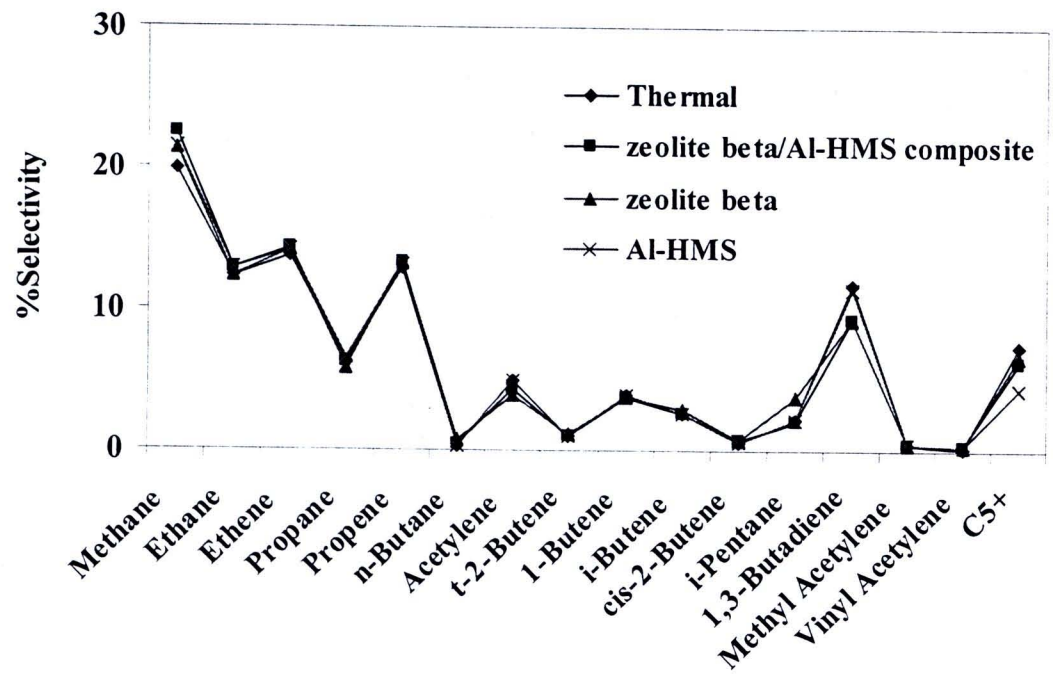

Figure 4.26 Distribution of gas fraction obtained by thermal and catalytic cracking of grease over Al-HMS, zeolite beta and zeolite beta/Al-HMS composite catalysts at 400°C for 120 min.

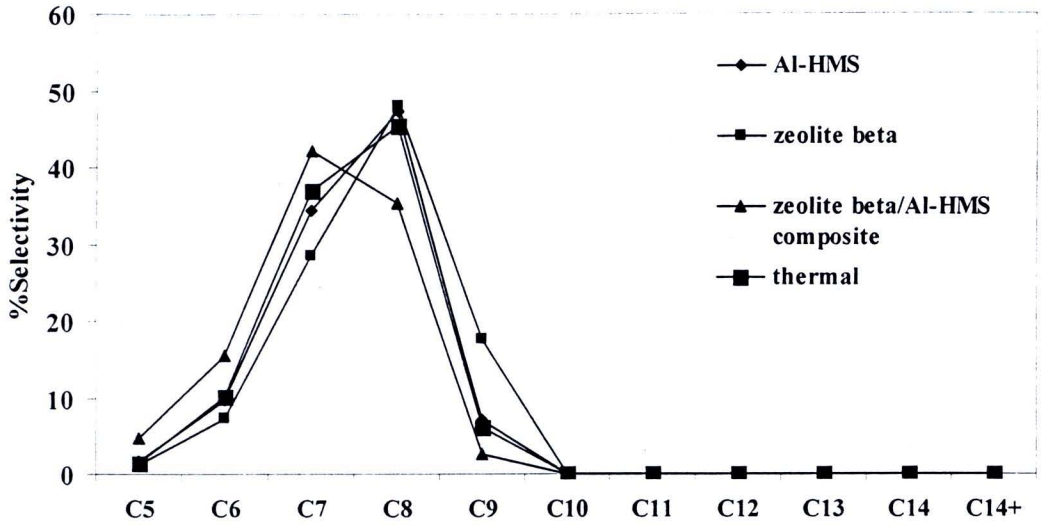

Figure 4.27 Carbon number distribution of distillate oil obtained by thermal and catalytic cracking of grease over Al-HMS, zeolite beta and zeolite beta/Al-HMS composite catalyst at 400°C for 120min.

Figure 4.27 showed the product distribution of distillate oil obtained by thermal cracking and catalytic cracking of grease over zeolite beta/Al-HMS composite catalyst at 400°C. All liquid products were composed of hydrocarbons in range of C_6-C_9 based on the boiling point range using n-paraffins as reference. For thermal and catalytic cracking of grease over Al-HMS and zeolite beta, liquid products were mainly in C_8 whereas that of composite catalyst was mainly in the range of C_7-C_8.

4.2.3 Conversion of polypropylene

4.2.3.1 Effect of the reaction times

The degradation of PP over zeolite beta/Al-HMS composite catalyst with Si/Al ratio in gel of zeolite beta of 60 was carried out at 350°C for 120 min. The accumulative volume of liquid fractions from catalytic cracking of PP over zeolite beta/Al-HMS composite catalyst was shown in Figure 4.28. The accumulative volume of liquid fraction was increased when the reaction time was increased. It was noticed that the total accumulative liquid volume seemed to be constant after 60 min. Then, the reaction times at 60, 90 and 120 min were investigated in this study. The results were summarized in Table 4.9. By increasing the reaction times from 60 to 120 min,

the %conversion was increased. With increasing the reaction time, a high conversion of PP into products was observed and resulted in the increase in yields of liquid and gas products whereas the residue yield decreased. It was suggested that zeolite beta/Al-HMS composite catalyst facilitated the cracking of PP into low molecular weight molecules. When the reaction time increased, PP had more time to react with the catalyst and produced more liquid and gas products until it seems to be constant. However, the accumulative volume of liquid fraction increasing with time but after 60 min the accumulative liquid volume was not much different. Therefore, the reaction time at 60 min was chosen for further study.

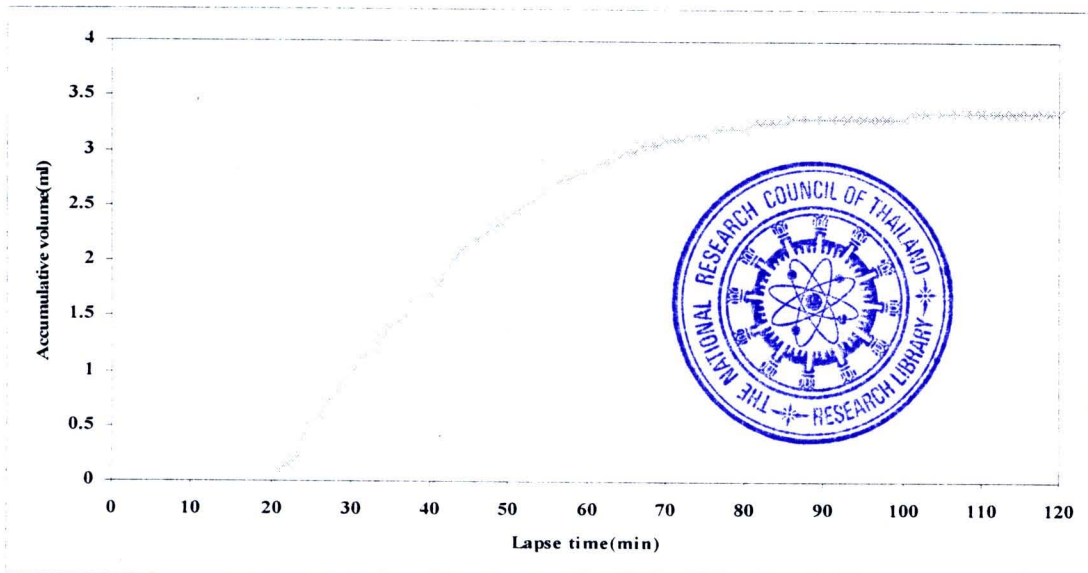

Figure 4.28 Accumulative volume of liquid fractions from catalytic cracking of PP over zeolite beta/Al-HMS composite catalysts at 350°C for 120 min.

Table 4.9 Catalytic cracking of PP over zeolite beta/Al-HMS composite catalysts catalyst with Si/Al ratio in gel of zeolite beta of 60 with various time

Reaction time	60 min	90 min	120 min
%Conversion*	73.8	83.7	95.0
%Yield* 1. gas fraction	31.6	38.7	47.8
2. liquid fraction	42.2	45.0	47.2
3. residue	26.2	16.3	5.0
Liquid fraction density (g/ cm^3)	0.78	0.78	0.78

Condition: N_2 flow of 20 cm^3/min, reaction temperature of 350°C, 10 wt% catalyst to PP. *Deviation within ± 0.9 for conversion, ± 0.5 for yield of gas fraction, ± 0.9 for yield of liquid fraction, and ± 0.9 for yield of residue.

4.2.3.2 Effect of the reaction temperatures

The influence of the reaction temperatures in the range of 350-400°C was investigated using zeolite beta/Al-HMS catalyst with Si/Al ratio in gel of zeolite beta of 60 and thermal reaction were also conducted as shown in Table 4.10. In order to find optimal reaction temperature for PP cracking, value of the %conversion was increased when the reaction temperatures was raised. It was obviously seen that the selectivity to gas and liquid products were increased. The high reaction temperatures enhanced the degradation of polymer *via* carbocation and free radicals mechanisms.

Figure 4.29 showed the accumulative volume of liquid fractions in the graduated cylinder increased as a function of lapsed time. When the temperature is increased, the initial rate of liquid fraction formation was much faster in order 400°C, 380°C and 350°C. However, the total volume of liquid fraction was no difference for 400°C compared to that at 380°C.

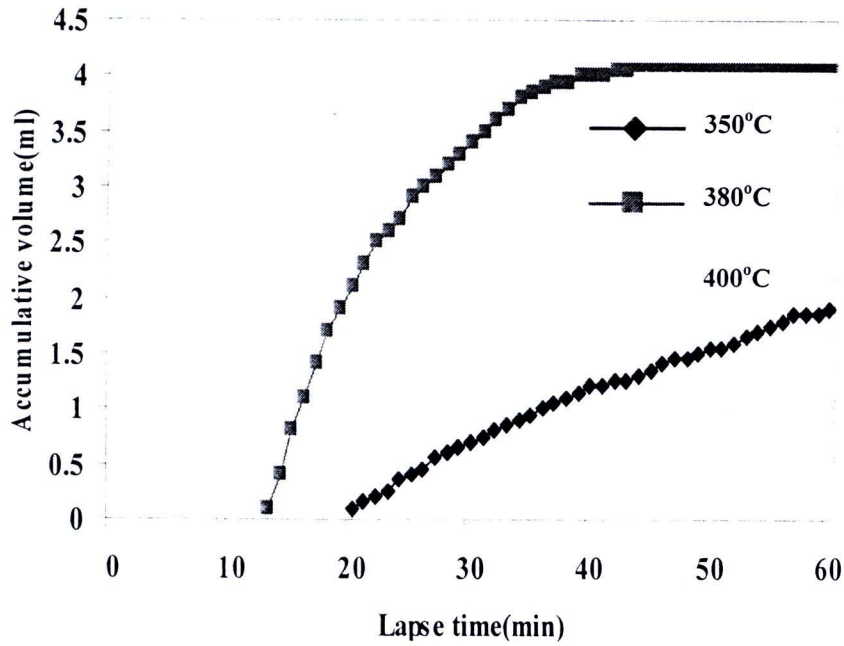

Figure 4.29 Accumulative volume of liquid fractions from catalytic cracking of PP over zeolite beta/Al-HMS composite catalysts at 350, 380 and 400°C for 60 min.

Comparing between thermal cracking and catalytic cracking at the same temperature, the catalytic cracking showed higher %conversion than thermal cracking because the acidity of catalyst increased the degradation of polymer. The

value of %conversion of zeolite beta/Al-HMS composite steeply increased from 60.20 to 95.20% when the reaction temperature increased from 350°C to 380°C and that remained constant for 96.40% at 400°C. The yields of both gas and liquid products are affected by the reaction temperatures. Considering at the reaction temperatures in range of 380°C to 400°C, the %yields of the liquid fraction and the gas fraction were about 57% and about 37-39%, respectively. The selectivity of distillate oil at 350°C and 380°C was higher than the selectivity of distillate oil at 400°C. Furthermore, the yields of distillate oil at 350°C and 380°C were 21.09 and 39.61, respectively. From this result, the composite catalyst showed the highest efficiency in cracking of PP at 380°C. Therefore, the reaction temperature at 380°C was chosen for further study.

Table 4.10 Thermal and catalytic cracking of PP over zeolite/Al-HMS composite catalyst at various temperatures for 60 min.

	Reaction temperatures					
	350°C		**380°C**		**400°C**	
	Thermal	**zeolite beta/AlHMS**	**Thermal**	**zeolite beta/AlHMS**	**Thermal**	**zeolite beta/AlHMS**
%Conversion*	2.4	60.2	62.8	95.2	90.6	96.4
%yield* 1. gas fraction	2.4	30.4	21.0	37.6	31.2	39.2
2. liquid fraction	-	29.8	41.8	57.6	59.4	57.2
3. residue	97.6	39.8	37.2	4.8	9.4	3.6
%selectivity of liquid fraction						
1. distillate oil (%yield of distillate oil)**	-	70.8 (21.09)	33.5 (14.00)	68.8 (39.61)	11.5 (6.48)	48.9 (27.9)
2. heavy oil	-	29.2	66.5	31.2	88.5	51.2
Liquid fraction density (g/ cm^3)	-	0.76	0.70	0.70	0.76	0.70

Condition: N_2 flow of 20 cm^3/min, reaction time of 60 min, 10 wt% of catalyst to PP. *Deviation within ± 0.9 for conversion, ± 0.5 for yield of gas fraction, ± 0.9 for yield of liquid fraction, and ± 0.5 for yield of residue. **% yield of distillate oil = % yield of liquid fraction × %selectivity of liquid fraction and divided by 100.

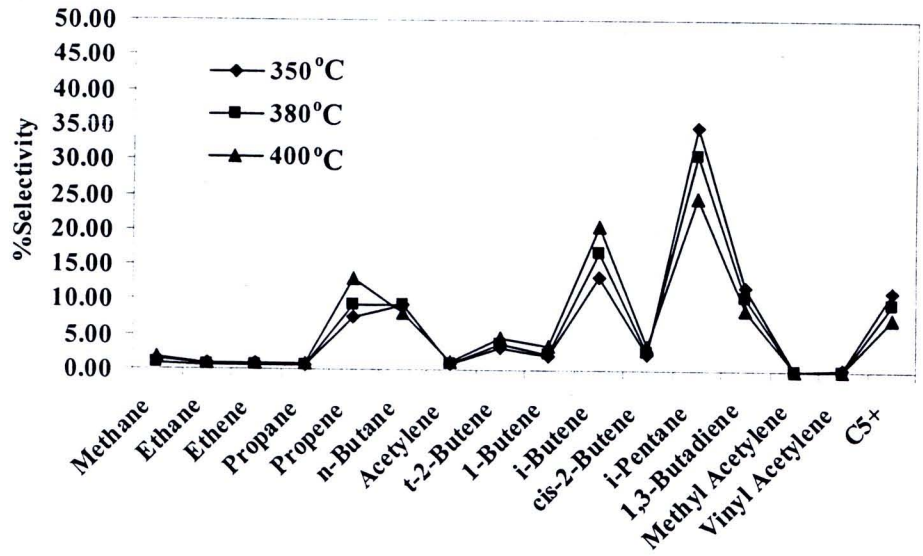

Figure 4.30 Distribution of gas fraction obtained by thermal and catalytic cracking of PP over zeolite beta/Al-HMS composite catalyst at various temperatures for 60 min.

Figure 4.30 showed distribution of gas fraction obtained by catalytic cracking of PP over zeolite beta/Al-HMS composite at 350°C, 380°C and 400°C. The compositions of gas fraction were the same and mainly consist of i-pentane, i-butene and C_5^+.

4.2.2.3 Effect of various catalyst

The %conversion and %yield of thermal and catalytic crackings of PP at 380°C for 60 min over Al-HMS (Si/Al=60), zeolite beta (Si/Al=60) and zeolite beta/Al-HMS composite catalyst with Si/Al ratio in gel of zeolite beta of 60 were showed in Table 4.11. Although, the %conversion of zeolite beta/Al-HMS composite was nearly reached to zeolite beta, gas fraction of zeolite beta was higher than gas yield of the composite catalyst. The specific surface area cannot explicate the activity of those catalysts because the specific surface area of both catalysts was not significantly different. The explanation of this result was the acidity of catalyst, as the acidity of zeolite beta was higher than the acidity of zeolite beta/Al-HMS composite. Accordingly, the gas product that archived by zeolite beta catalyst gave the quantity of small molecules more than the composite catalyst. The zeolite beta/Al-HMS composite catalyst gave the selectivity and yield of distillate oil more than zeolite beta

catalyst. This result indicated that pore size of zeolite beta/Al-HMS composite had small pore, which enhanced small molecules to react in the pores and gave high distillate oil. This result could be explained by acidity of catalyst. The acidity of composite catalyst was less than zeolite beta, therefore, the gas product that achieved by zeolite beta gave the amount of small molecules more than the zeolite beta.

The value of %conversion over Al-HMS and the composite catalyst was similar. However, gas fraction of Al-HMS was less than gas fraction of composite catalyst. This result could be explained by acidity of catalyst, as the acidity of Al-HMS was less than composite catalyst. Therefore, the gas product that achieved by composite catalyst gave the amount of small molecules more than the Al-HMS catalyst. On the other hand, liquid fraction of Al-HMS was higher than composite catalyst because Al-HMS had larger pore size and channels allowed the formation of higher hydrocarbon products than the composite catalyst.

The %conversion of Al-HMS was only slightly more than that of, zeolite beta but the selectivity to distillate oil of Al-HMS was selectivity higher than zeolite beta. These results could also be explained by the structure and properties of catalyst materials. Al-HMS had surface area at 843 m^2/g with a wide pore size of 4.19 nm, whereas zeolite beta had lower surface area at 737 m2/g with a pore size of 0.6 nm. The large pore size of Al-HMS allowed large polymer molecules to access the pore better than zeolilte beta, resulting high conversion of PP and high liquid product.

The composition of gaseous products from PP cracking at 380°C was shown in Figure 4.31. The gas fraction obtained by thermal cracking consisted of 1,3-butadiene, propene and $C5^+$. For catalytic cracking, the gas components obtained from cracking of composite catalyst were similar to those of Al-HMS and zeolite beta catalyst. The major components were i-pentane, 1-butene and $C5^+$.

Table 4.11 Thermal and catalytic cracking of PP over Al-HMS, zeolite beta and zeolite/Al-HMS composite catalyst at 380°C for 60 min.

	Reaction temperature at 380°C			
	Thermal	**Al-HMS**	**Zeolite beta**	**Zeolite beta/AlHMS**
%Conversion*	62.8	96.6	95.4	95.2
%Yield* 1. gas fraction	21.0	23.0	48.2	37.6
2. liquid fraction	41.8	70.6	47.2	57.6
3. residue	37.2	6.4	4.6	4.8
%Selectivity of liquid fraction				
1. distillate oil (%yield of distillate oil)**	33.5 (14.00)	36.3 (25.29)	35.7 (16.84)	68.8 (39.64)
2. heavy oil	66.5	63.7	64.3	31.2
Liquid fraction density (g/cm^3)	0.70	0.72	0.70	0.70

Condition: N_2 flow of 20 cm^3/min, reaction temperature of 380°C for 60 min, 10 wt% of catalyst to PP. *Deviation within ± 0.9 for conversion, ± 0.5 for yield of gas fraction, ± 0.9 for yield of liquid fraction, and ± 0.5 for yield of residue. **% yield of distillate oil = % yield of liquid fraction × %selectivity of liquid fraction and divided by 100.

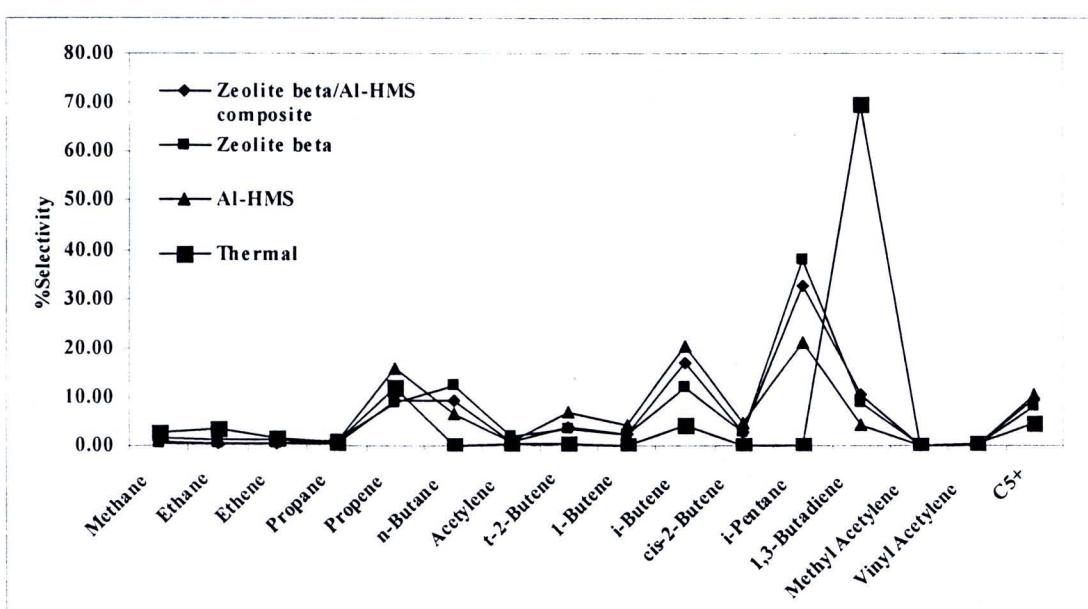

Figure 4.31 Distribution of gas fraction obtained by thermal and catalytic cracking of PP over Al-HMS, zeolite beta and zeolite beta/Al-HMS composite catalyst at 380°C for 60 min.

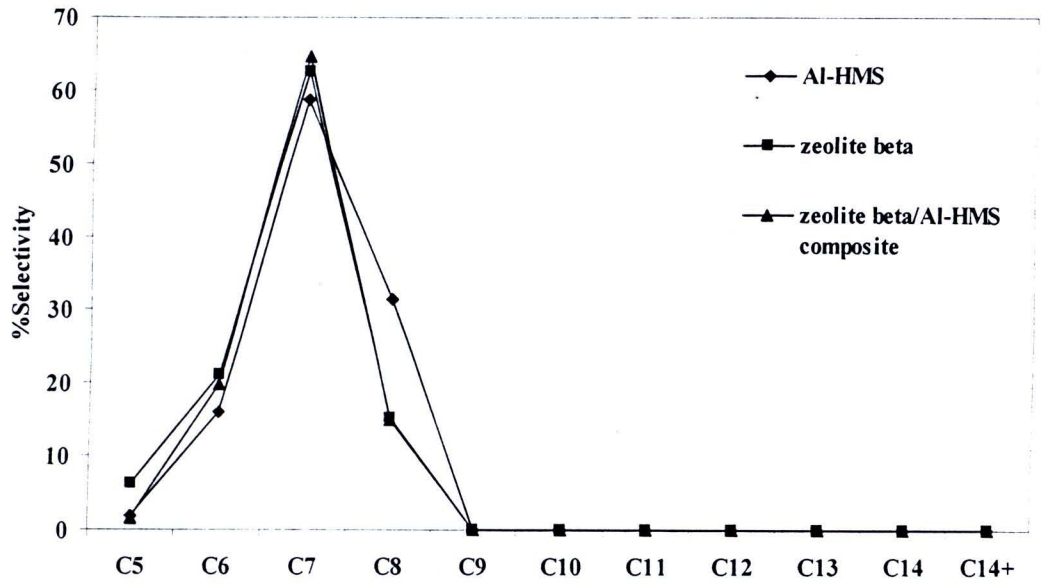

Figure 4.32 Carbon number distribution of distillate oil obtained by catalytic cracking of PP over Al-HMS, zeolite beta and zeolite beta/Al-HMS composite catalyst at 380°C for 60 min.

Figure 4.32 showed the product distribution of distillate oil obtained by catalytic cracking of PP over zeolite beta/Al-HMS composite at 380°C for 60 min. All liquid products were mainly in C_7.

4.2.3.4 Effect of Si/Al ratio

The zeolite beta/Al-HMS composite catalyst with various Si/Al ration in gel of zeolite beta (40, 60 and 120 respectively) and thermal cracking were tested in degradation of PP at temperature of 380°C for 60 min. Considering the data in Table 4.12, %conversion of thermal cracking at 380°C was only 62.8%. For the catalytic cracking over zeolite beta/Al-HMS catalysts, the %conversion was increased from 62.8 wt% to about 93-95 wt% compared with thermal cracking. The result indicated that the waxy residue decomposed into relatively lighter liquid hydrocarbons resulting in higher yield of liquid fractions than the case of thermal cracking. Considering the increase of the aluminum content in composite catalysts, the %conversion was not significantly different. However, the liquid fraction was decreased when the aluminum content was reduced.

Table 4.12 Thermal and catalytic cracking of PP over zeolite/beta composite with various Si/Al ration.

	Thermal	Composite40	Composite60	Composite120
%Conversion*	62.8	93.4	95.2	94.6
%yield* 1. gas fraction	21.0	33.6	37.6	39.2
2. liquid fraction	41.8	59.8	57.6	55.4
3. residue	37.2	6.6	4.8	5.4
%selectivity of liquid fraction				
1. distillate oil (%yield of distillate oil)**	33.5 (14.00)	60.0 (35.88)	68.8 (39.61)	65.0 (36.01)
2. heavy oil	66.5	40.0	31.2	35.0
Liquid fraction density (g/cm^3)	0.77	0.77	0.76	0.76

Condition: N_2 flow of 20 cm^3/min, reaction temperature of 380°C, 10 wt% catalyst to PP. *Deviation within ± 0.9 for conversion, ± 0.8 for yield of gas fraction, ± 1.1 for yield of liquid fraction, and ± 0.8 for yield of residue.

**% yield of distillate oil = % yield of liquid fraction x %selectivity of liquid fraction divided by 100.

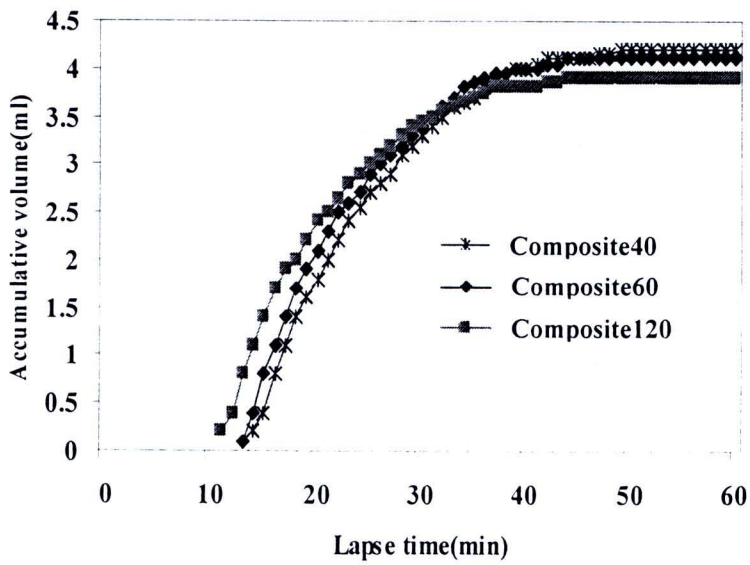

Figure 4.33 Accumulative volume of liquid fractions from catalytic cracking of PP over zeolite beta/Al-HMS composite catalyst with various Si/Al ration in gel of zeolite beta 40, 60 and 120 at 380°C for 60 min.

Figure 4.33 showed the accumulative volume of liquid fractions in the reaction. It was seen that the rate of liquid formation of over zeolite beta/Al-HMS composite catalyst with Si/Al ration in gel of zeolite beta 120 was faster than 60 and 40 respectively. However, the total volume of liquid fraction was no difference for 60 compared to that at 120.

Figure 4.34 showed distribution of gas fraction obtained by catalytic cracking of PP over zeolite beta/Al-HMS composite catalyst with various Si/Al ration in gel of zeolite beta 40, 60 and 120 at 380°C for 60 min. The compositions of gas fraction were the same and mainly consist of i-pentane, i-butene and propene.

Figure 4.35 showed the product distribution of distillate oil obtained by catalytic cracking of PP over zeolite beta/Al-HMS composite catalyst with various Si/Al ration in gel of zeolite beta of 40, 60 and 120 at 380°C for 60 min. All liquid products were mainly in C_7.

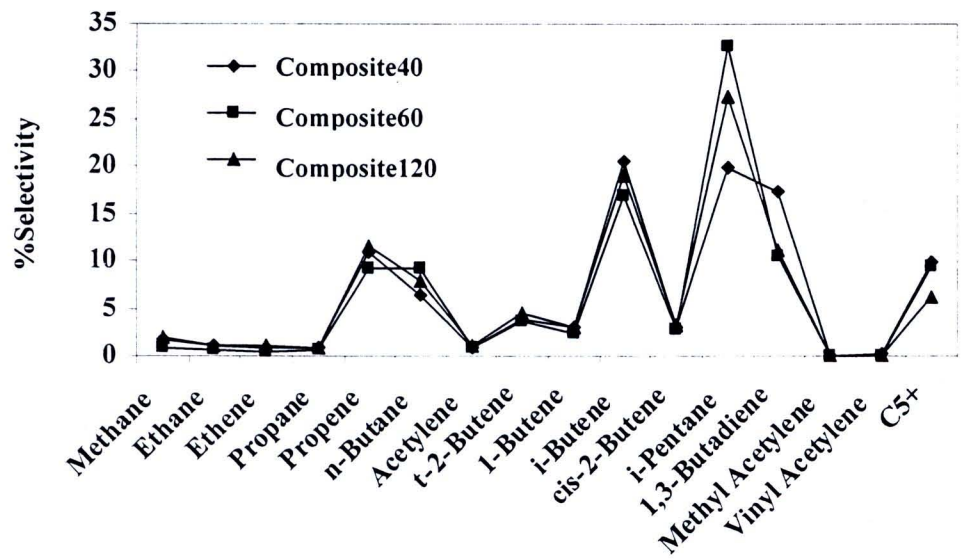

Figure 4.34 Distribution of gas fraction obtained by catalytic cracking of PP over zeolite beta/Al-HMS composite catalyst with various Si/Al ration in gel of zeolite beta 40, 60 and 120 at 380°C for 60 min.

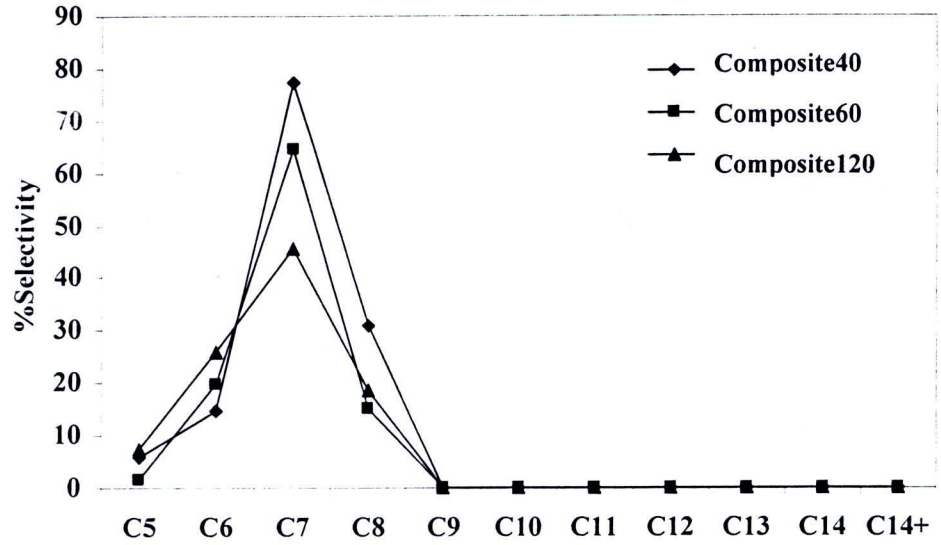

Figure 4.35 Carbon number distribution of distillate oil obtained by thermal and catalytic cracking of PP over zeolite beta/Al-HMS composite catalyst with various Si/Al ration in gel of zeolite beta 40, 60 and 120 at 380°C for 60 min.

4.2.4 Catalyst regeneration

The zeolite beta/Al-HMS composite catalyst became black after the reaction due to deposition of coke on the surface and in the pores. However, it easily turned to white after regeneration by calcination in a muffle furnace at 500°C for 5 h. Thus, the zeolite beta/Al-HMS composite catalyst with Si/Al ratio in gel of zeolite beta of 60 was used in this study. The regenerated composite catalysts were characterized using XRD and nitrogen adsorption-desorption techniques. Then, the catalytic test for regenerated catalyst was performed at the optimal condition. Figure 4.36 showed XRD patterns of the freshly calcined and the regenerated zeolite beta/Al-HMS catalysts. After the catalytic run, both structures of microporous and mesoporous were still remained for the 1stregenerated, 2nd regenerated and 3rd regenerated catalysts. The crystallinity of composite at small angle was decreased after the first run whereas those at wide angle were not different, suggesting that crystallinity of HMS structure slightly decreased. Moreover, comparable with the physical mixing, as in the previous research report by N. Kache [65], it seem that the structure of the composite catalyst more stable than physical mixing catalyst, due to the mesoporous structure (low angle) of physical mixing catalyst dramatically decreased. All samples gave a typical

isotherm of type IV. The BET specific area of 1st regenerated, 2nd regenerated and 3rd regenerated catalysts were 538, 532 and 516m^2/g, respectively. They were slightly lower compared with the fresh catalyst (671m^2/g). Then, the catalytic test for regenerated catalyst was performed at the 380°C for 60 min.

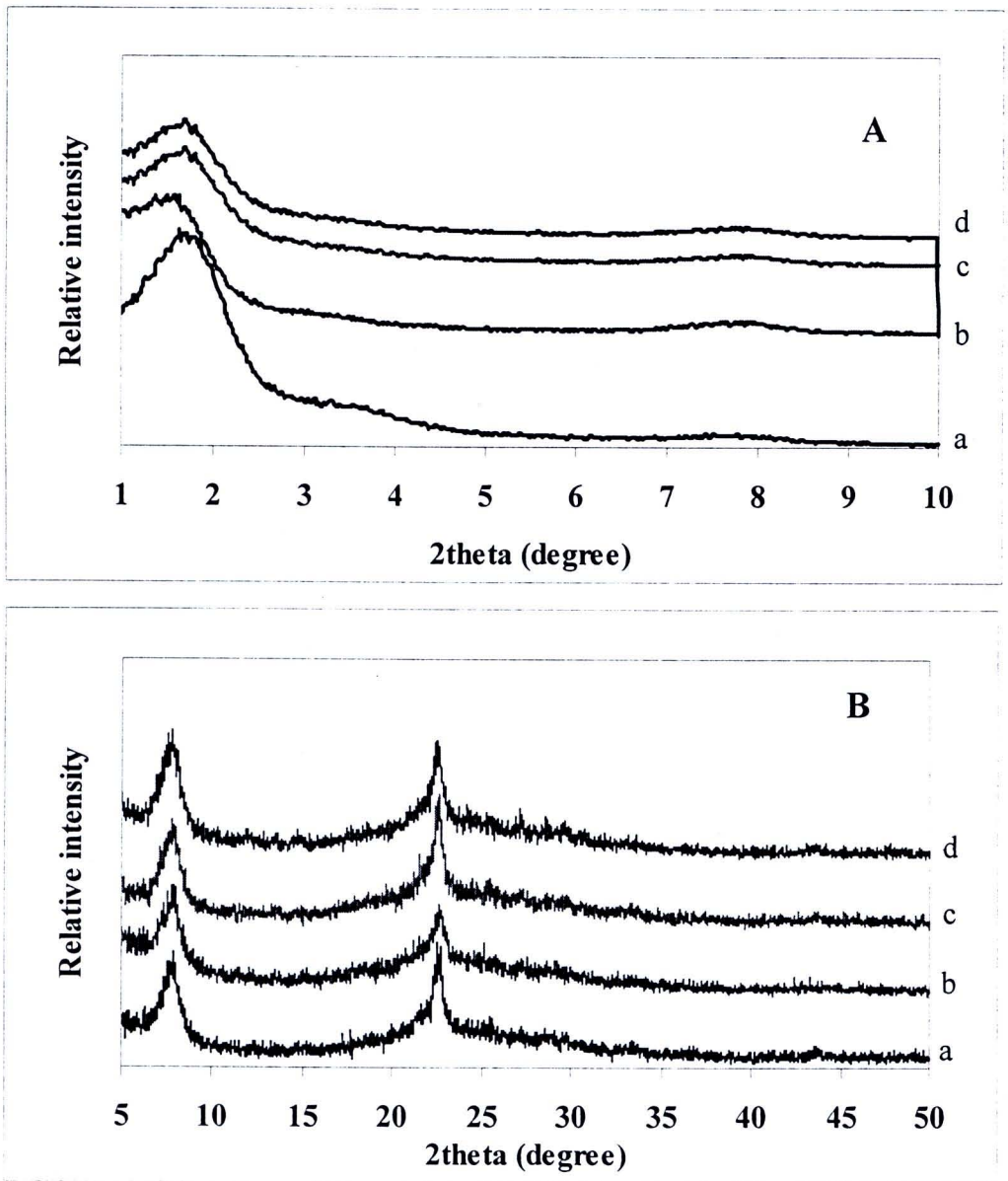

Figure 4.36 XRD patterns of zeolite beta/Al-HMS composite catalyst with Si/Al ratio in gel of zeolite beta of 60 (a) fresh, (b) 1st regenerated, (c) 2nd regenerated, and (d) 3rd regenerated at small angle (A) and wide angle (B) degree.

Table 4.13 summarized the values of %conversion and product yield obtained from the PP cracking over fresh and regenerated zeolite beta/Al-HMS catalyst with Si/Al ratio in gel of zeolite beta of 60 at 380 °C for 60 min. The values of %conversion obtained in the cracking over regenerated catalyst were not different from fresh catalyst. There were no differences between the yield of gas and liquid faction of fresh and regenerated catalyst, whereas the 3rd regenerated catalyst provided lower selectivity of distillate oil comparing to the fresh catalyst. This result might be because the regenerated catalyst had less specific surface area than the fresh catalyst. It was also illustrated that in the cracking of C-C bonds, the specific surface area of catalysts plays an important role; primary cracking reactions of polymer chain proceed on the macroporous surface of the catalyst, while the smaller fragments are cracked on their micropore surface.

Table 4.13 Catalytic cracking of PP using the fresh and the regenerated zeolite beta/Al-HMS composite catalyst with Si/Al ratio in gel of zeolite beta of 60.

Type of catalysts	Fresh	1st regenerated	2 nd regenerated	3 rd regenerated
%Conversion*	95.2	95.6	94.8	94.2
%yield* 1. gas fraction	37.6	35.8	35.2	38.0
2. liquid fraction	57.6	59.8	59.6	56.2
3. residue	4.8	4.4	5.2	5.8
%selectivity of liquid fraction				
1. distillate oil (%yield of distillate oil)**	68.8 (39.62)	67.5 (40.36)	63.8 (38.02)	55.4 (31.13)
2. heavy oil	31.3	32.50	36.2	44.6
Liquid fraction density (g/cm^3)	0.70	0.71	0.70	0.70

Condition: N_2 flow of 20 cm^3/min, reaction temperature 380 °C for 60 min, 10 wt% catalyst of plastic. *Deviation within 0.8% for conversion, 0.6% for yield of gas fraction, 0.9% for yield of liquid fraction, and 0.7% for yield of residue. Only one reaction was performed for 3 rd regenerated catalyst because there was not enough reused catalyst for the reaction divided by 100.

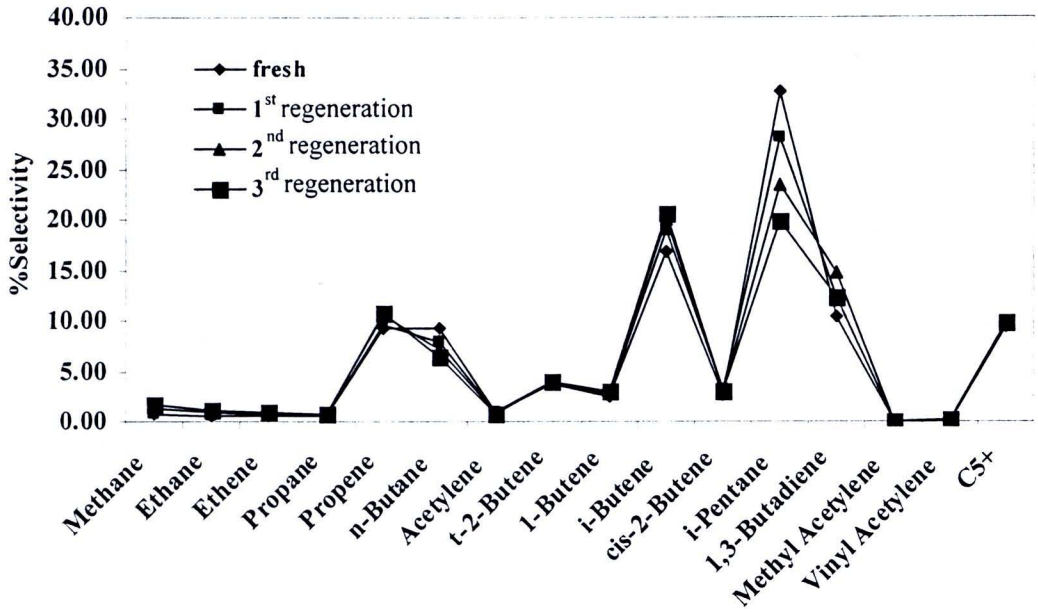

Figure 4.37 Distribution of gas fraction obtained by catalytic cracking of PP over fresh and the regenerated zeolite beta/Al-HMS composite catalyst.

The distribution of gas components formed in PP cracking over the fresh and the regenerated zeolite beta/Al-HMS composite catalysts at 380°C were given in Figure 4.37. The gas fraction of all reactions composed of similar hydrocarbon products but for fresh catalyst, the selectivity to i-pentane was higher than the regenerated catalysts. The mainly gas fraction from PP were i-pentane, i-butene and propene.

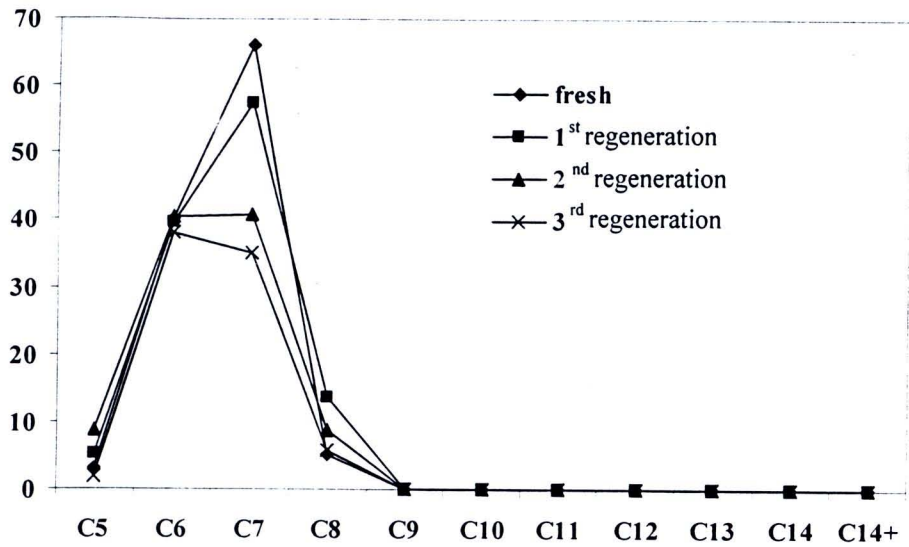

Figure 4.38 Carbon number distributions of liquid fraction obtained by catalytic cracking of PP using the fresh and the regenerated zeolite beta/Al-HMS composite catalyst.

Figure 4.38 showed the product distribution of distillate oil obtained by the PP cracking using the fresh and regenerated zeolite beta/Al-HMS composite catalyst 380°C. Both fresh and 1st regenerated catalyst provided mainly C_7. For 2nd regenerated and 3rd regenerated catalyst, the liquid fractions were mainly C_6 and C_7.

In this section, it was concluded that the composite used catalyst could be regenerated easily in a furnace. Its cracking activity was acceptable due to a high conversion in PP cracking over 90%. The distribution of gas product was similar to the fresh catalyst.